Chemical Papers (2018) 72:1823–1851
https://doi.org/10.1007/s11696-018-0411-0

REVIEW

Fluorescent and colourimetric 1, 8-naphthalimide-appended chemosensors for the tracking of metal ions: selected examples from the year 2010 to 2017

Stephen O. Aderinto[1] · **Sarah Imhanria**[1]

Received: 21 July 2017 / Accepted: 2 February 2018 / Published online: 27 February 2018

Abstract
The global sensing science in the past couple of years has seen brilliant successes in the designs and syntheses of diverse fluorescent and colourimetric chemosensors of ultra-high selectivities and sensitivities for the tracking of metal ions in environmental and biological systems. Amongst the most widely employed fluorophores for the development of fluorescent and colourimetric chemosensors is the 1, 8-naphthalimide fluorophore, which is distinctive due to its possession of outstanding photophysical properties unequalled by other fluorophores. Many reported literatures are replete with employment of 1, 8-naphthalimide as a unique fluorophore for the construction of chemosensors for the monitoring of metal ions (such as Cu^{2+}, Hg^{2+}, Cr^{3+}, Fe^{3+}, Zn^{2+}, Ag^{+}, Pd^{2+}, Al^{3+}, Ba^{2+}, Au^{3+}, and Bi^{2+}, and/or a combination of any of them) with remarkable results documented from various labs. This review summarises recent advances in the development of representative fluorescent and colourimetric 1, 8-naphthalimide-based chemosensors reported within the past 7 years. It is believed that gaining insights into the various highlighted examples would help to refine our knowledge of the field and pave the way for further advancement in the constructions of fluorescent and colourimetric 1, 8-naphthalimide-based chemosensors of improved sensing parameters and practical application values.

Keywords Fluorescent and colourimetric chemosensors · Metal ions · Fluorophore · 1, 8-Naphthalimide · Photophysical properties

Introduction

Over the past two decades of the advent of the supramolecular chemistry, research efforts have been directed towards the development of fluorescent chemosensors as vibrant tools for sensing various heavy metal ions and anions of environmental and biological significance, and hydrogen ion (i.e. proton) in biological systems (Gunnlaugsson et al. 2006; Lodeiro and Pina 2009; Duke et al. 2010; Georgiev et al. 2011; Marinova et al. 2011). Inasmuch as the fluorescent technique is a very useful sensing tool, it has enjoyed wide application in the research areas of clinical diagnostics, biotechnology, molecular biology and biochemistry, and materials and environmental sciences (Mason 1999; Lakowicz et al. 2006). The fluorescent signalling method offers the multiple advantages of high sensitivity and selectivity, real-time monitoring, local observation, simplicity of operation, inexpensiveness of equipment, and fast response time (Lee et al. 2015; Carter et al. 2014; Zhang et al. 2014a; Kim et al. 2012), and non-destructibility, that overrule the merits of extant traditional bulk methods of high-performance liquid chromatography, mass spectrometry, and atomic absorption spectroscopy. A closely related detection technique to fluorescence method is colourimetric method, which has also been used as a powerful sensing tool because it can afford naked eye detection even before the use of spectrophotometric analysis. The method has been successfully used in diagnostic assays like blood-glucose monitoring and early pregnancy tests (Bicker et al. 2011).

✉ Stephen O. Aderinto
2014bsz528@stu.lzjtu.edu.cn; stephen_aderinto@yahoo.com

Sarah Imhanria
sarahimha@gmail.com

[1] School of Chemical and Biological Engineering, Lanzhou Jiaotong University, Lanzhou 730070, Gansu, People's Republic of China

Fluorescent chemosensors

Also known as probes, generally, chemical sensors or chemosensors are molecules that are capable of detecting matter or energy with the concomitant output of a signal that could be measured. Sensors which upon interaction with a species under test (i.e. an analyte) give fluorescence modulations are grouped collectively as fluorescent chemosensors. Typically, chemosensors are made up of three components and are usually designed on the 'fluorophore–spacer–receptor' paradigm (Bryan et al. 1989) as illustrated in Fig. 1. Given their differences, each component of a chemosensor serves distinct role as briefly explained below (Parkesh et al. 2011; de Silva et al. 1995a; Wasielewski 1992):

The fluorophore

The fluorophore is the signalling moiety and is responsible for the transduction of the interaction between the receptor and the species being detected (i.e. analyte) into a readable signal of change in fluorescence. Chemosensors owe their colours to the structural features of the fluorophore moieties they embed. Commonly encountered fluorophores include boron-dipyrromethene (BODIPY), rhodamine, fluorescein, pyrene, anthracene, naphthalimide, and coumarin (Deng et al. 2017; Liu et al. 2017b; Papalia et al. 2017; Dey et al. 2017; Jiang et al. 2017; Mironenko et al. 2017; Erdemir and Kocyigit 2017; Fu et al. 2017a; Hou et al. 2017; Goncalves et al. 2017a; Sun et al. 2017; Saura et al. 2017; Gupta et al. 2017; Liu et al. 2017b; Gonçalves et al. 2017b; Huang et al. 2017).

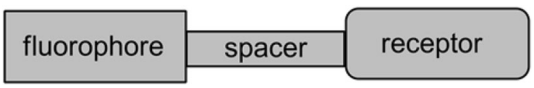

Fig. 1 The paradigm for a fluorescent chemosensor (a spacer may or may not be present)

The spacer

The spacer links and keeps both the fluorophore and receptor at a convenient distance to allow for the feasibility of photoinduced electron transfer (PET) process which dictates the tunable fluorescence property of fluorescent chemosensors. Chemosensors necessarily may or may not anchor spacer. Most commonly encountered length of a spacer is a few carbon chains usually between a single to a double carbon chain.

The receptor

This is also known as the recognition unit, and it serves the purpose of binding to the analyte in a way that allows for selectivity and effectiveness.

The process whereby chemosensors interact with an analyte species to give off an energy that could be measured is known as signal 'transduction'. The fluorescence mechanism is one such desirable transduction mechanism since the emission wavelength always displays higher value than that of the excitation wavelength. Low concentrations of analyte substances are required for such signalling transduction. Figure 2 gives a diagrammatic illustration of typical fluorescence signal transduction mechanism (de Silva et al. 1995a).

Ideally, fluorescent chemosensors must fulfil two stringent requirements: on the one hand, there must be enough affinity between the receptor unit and the relevant analyte; on the other hand, there must be no interferences from the other rival substances under the same investigation (Valeur and Leray 2001).

The 1, 8-naphthalimide fluorophore

To date, several fluorophores have been widely used in the construction of fluorescent chemosensors, including

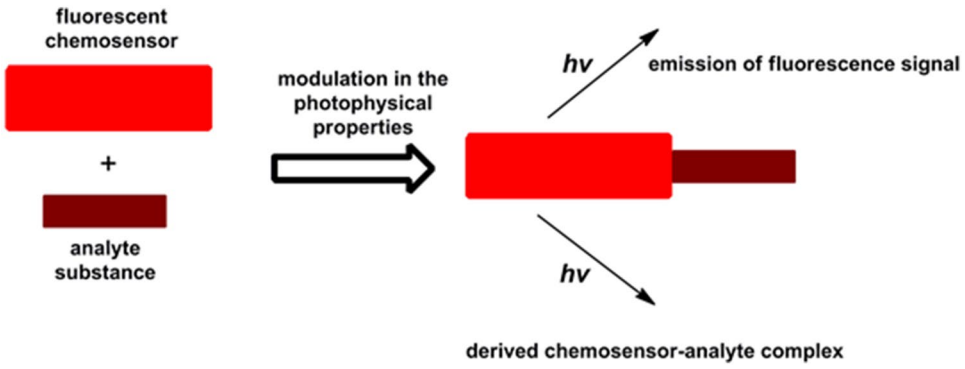

Fig. 2 Schematic illustration of the photophysical changes ensuing from the interaction between a fluorescent chemosensor and an analyte substance

boron-dipyrromethene (BODIPY), rhodamine, fluorescein, pyrene, anthracene, naphthalimide, coumarin, etc.). Amongst them, 1, 8-naphthalimide stands out as a much sought-after, exquisite fluorophore owing to its superior features of strong absorption band in the visible region (a wide range usually between 350 and 450 nm but can extend up to 650 nm), outstanding photostability, high fluorescent quantum yield (a wide range typically between 0.20 and 0.80), and large Stokes' shift (a wide range usually between 3500 and 6500 cm^{-1}), besides the possibility of an easy modification of its structure (Lippert et al. 2011; Shao et al. 2015; Lee et al. 2013; Du et al. 2012; Huang et al. 2014a; Lee et al. 2014; Shaki et al. 2010). 1, 8-naphthalimide contains a very strong naphthalene ring structure so that the interaction of its molecules with solvents or other solute molecules is reduced, making the external transfer energy to also be lowered, which is very beneficial to the emission of fluorescence. The presence of an electron donor conjugated system in its molecular structure allows for electrons in its system to be easily excited by the external light or electric field so as to produce a strong fluorescence (Grabchev et al. 1995). Owing to its conjugated electron system (i.e. π electron system), the 1, 8-naphthalimide structure could be easily modified via different synthetic approaches. This property can then be taken advantage of to interact with various substituents, thereby generating varied fluorescent transduction and properties. Figure 3 gives the structure of the 4-amino-1, 8-naphthalimide, which is the more commonly employed architectural block, although the 3-amino-1, 8-naphthalimide unit is also occasionally used (de Silva et al. 1996).

Having been validated to be a fantabulous fluorophore, there have been several instances of engagement of 1, 8-naphthalimide as a key component in the design of fluorescent dyes for polymer materials (Bojinov and Grabchev 2003), laser active media (Gruzinskii et al. 1998), fluorescent markers in biology (Stewart 1981), anticancer agents (Ott et al. 2008) and medicinal analgesics (de Souza et al. 2002), fluorescence switches and sensors (Bojinov et al. 2009), light emitting diodes (Liu et al. 2006), electroluminescent materials (Zhu et al. 2003) liquid crystal displays (LCDs) (Grabchev and Chovelon 2003a), ion probes (Cosnard and Wintgens 1998), logic gates (de Silva et al. 1997b), and organic photoconductive materials (Law 1993).

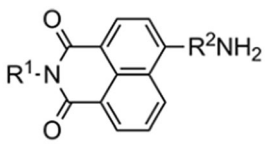

R^1 could be a hydrogen or an alkyl group
R^2 is an alkyl group

Fig. 3 The structure of 1, 8-naphthalimide fluorophore with atom numbering showing the 1 and 8 positions and an amino group at the 4-position bearing the imide nitrogen atom

Over the years, there are a plethora of fluorescent chemosensors built from the 1, 8-naphthalimide fluorophore for the monitoring of metal ions. Such exist in previous publications (de Silva et al. 1995b; Rurack et al. 2000; Burdette et al. 2001; Grabchev et al. 2003b; Gunnlaugsson et al. 2003; He et al. 2003; Fan et al. 2005; Bricks et al. 2005; Wang et al. 2005; Liu et al. 2005; Xu et al. 2005; Anikin and Fedko 2006; Cosnard and Wintgens 1998; Xu et al. 2006; Lu et al. 2007; Chovelon et al. 2007; Mu et al. 2007; Parkesh et al. 2007; Staneva et al. 2007; Grabchev et al. 2004; Bojinov et al. 2008; Grabchev and Chovelon 2008; Duan et al. 2008; Tamanini et al. 2009; Li et al. 2009; Bojinov and Panova 2009; Nandhikonda et al. 2009). It should be made known that it is not the attempt of this review to revisit those pretty 'old' references but to report the 'newer' ones within the past seven years, i.e. between the years 2010 and 2017. Enough references, 76 articles thereabout, have been reviewed in strength so as to bring to the research spotlight the tremendous works that have done in this field but at the same time ensure conciseness of the report. Moreso, the works reported focus on some representative metal ions, including but not limited to Cu^{2+}, Hg^{2+}, Zn^{2+}, Ag^{+}, Pd^{2+} and Au^{3+}, and/or a combination of them. Restriction has been placed on the 1, 8-naphthalimide as the fluorophore, with various receptors been successfully coupled with it. All reported compounds either make use of the fluorescence method or combined fluorescence and colourimetry method in their detection modes. To the best of the author's knowledge, such a recently published review of various 1, 8-naphthalimide-based chemosensors for different cations within the 7-year duration has not been reported.

Metal-specific 1, 8-naphthalimide-based fluorescent chemosensors

Cation sensing has been one of the principal goals and pursuits of researchers in the field of supramolecular chemistry owing to the indisputable roles and impacts of cations in our day-to-day life. The environmental and biological relevance of cations have been recognised (de Silva et al. 1997a; Xiao et al. 2007; Que et al. 2008; Kim et al. 2008; Xu et al. 2010c; Zhang et al. 2011b; Kim et al. 2012). This section maps out selected fluorescent and colourimetric 1, 8-naphthalimide-based chemosensors developed so far for cations.

Cu^{2+} ion-selective chemosensors

The research team of Fu et al. made remarkable success in the synthesis of the chemosensor **1** that bears 1, 8-naphthalimide Schiff base and photochromic diarylethene units

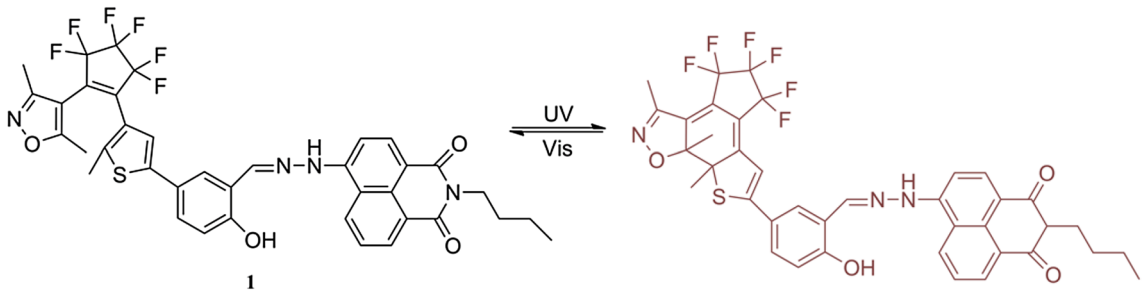

Fig. 4 Structure of **1** showing its UV–vis photochromism

(Fig. 4) (Fu et al. 2017b). This compound which exhibited both fluorescent and colourimetric signalling modes effectively discriminated Cu^{2+} ion from other cations present together in acetonitrile solution with association constant and detection limit calculated to be 3.13×10^4 and 2.4×10^{-6} mol L^{-1}, respectively. Insight into the Job's plot analysis yielded a 1:1 binding ratio. The synthesised compound was also capable of monitoring F^-. Despite all its other interesting features, the sensing mechanism of the reported compound was analytically irreversible.

In their recent work, the research group of Gao developed the water-soluble fluorescent chemosensor **2**, which anchors 1, 8-naphthalimide and two [12]aneN_3 as fluorophore moieties (Gao et al. 2016). The compound (Fig. 5) displayed high selectivity and sensitivity for Cu^{2+} ion monitoring in coexistence with several other ions investigated under the same conditions in Tris–HCl buffer system. Furthermore, the chemosensor experienced a quenching of its fluorescence upon binding with Cu^{2+} ion (a 127-fold dampening). As given by the titration experiment and Job's plot, its stoichiometric ratio of binding with Cu^{2+} ion was 1:2. In further experiment, the resultant complex **2**-Cu^{2+} was employed for the sensing of Adenosine-5′-triphosphate (ATP). The detection limits of chemosensor **2** towards Cu^{2+} ion and **2**-Cu^{2+} complex towards ATP were obtained to be 1.3×10^{-8} and 8.5×10^{-9} M, respectively, while the respective quantum yields of complex **2**-Cu and complex **2**-Cu with ATP were calculated to be 0.0014 and 0.1588. The most interesting features of **2** are its regeneration potency (i.e. capability to reversibly detect Cu^{2+} ion) upon the addition of ATP and its ability for Cu^{2+} ion and ATP monitoring in living cell samples.

Stimulated by the interesting fluorescent properties of 1, 8-naphthalimide fluorophore, Chen et al. designed and

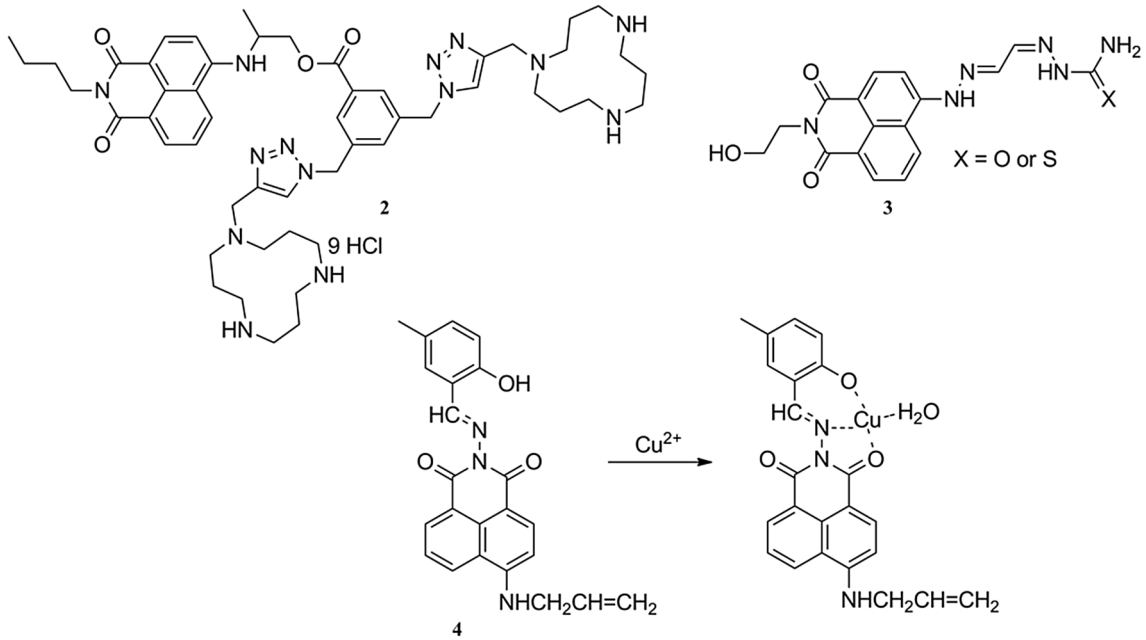

Fig. 5 Structures of **2** and **3** (up) and structure of **4** showing its binding mechanism with Cu^{2+} (down)

synthesised the simple but effective fluorescence 'turn on' chemosensor **3** (Chen et al. 2016). Noteworthy is that the chemosensor displayed an ultra-high sense of affinity towards Cu^{2+} in the mixture of other various metal ions tested in acetonitrile/water (50/50, v/v, 10 mM HEPES buffer, pH 7.4) solution. The binding ratio of the interaction of **3** and Cu^{2+} was established to be 1:1, and the detection limit was calculated as 0.0326 μM. The binding of the chemosensor with Cu^{2+} was demonstrated to be reversible. Finally, the chemosensor (Fig. 5) was applied for Cu^{2+} imaging in living cells.

Compound **4**, which anchors a 1, 8-naphthalimide unit as the fluorophore group and a Schiff base unit as the recognition group, was developed by Xu's research group as an efficient chemosensor for Cu^{2+} tracking (Fig. 5) (Xu et al. 2017). The chemosensor's performance was optimal at pH = 7.2. In Tris–HCl (pH = 7.2) buffer–DMF (1 : 1, v/v) solution, chemosensor **4** displayed unique selectivity for Cu^{2+} ion amongst other co-existed alkali, alkaline earth, and transition metal ions with a marked reduction in the fluorescence intensity of **4**. Job plot and fluorescence titration experiments revealed the formation of a 1:1 complex between **4** and Cu^{2+} ion. The chemosensor worked best for Cu^{2+} quantification within the linear range of 0.5–5 μM with detection limit and association constant of 0.23 μM and $1.328 \times 10^6\ M^{-1}$, respectively obtained.

He et al. fabricated a new naphthalimide-based fluorescent chemosensor, **5**, for the analytical detection of Cu^{2+} ion (Fig. 6) (He et al. 2015). In the absence of Cu^{2+} ion, **5** displayed strong greenish fluorescence. Upon the addition of 2 equiv. of Cu^{2+} ion to **5** in CH_3CN:H_2O (4:1, v/v) solution, there was disappearance of the greenish fluorescence with a simultaneous lowering of the emission intensity (a 30-fold quenching). The addition of other metal ions left a mild influence on the fluorescence intensity of **5**. Results of the Benesi-Hildebrand plot and ESI–MS spectra gave a 1:2 stoichiometric binding ratio of **5** with Cu^{2+}. The detection limit of **5** for Cu^{2+} detection was estimated to be 64 ppb. The compound was successfully assessed for practical detection of Cu^{2+} in living cells.

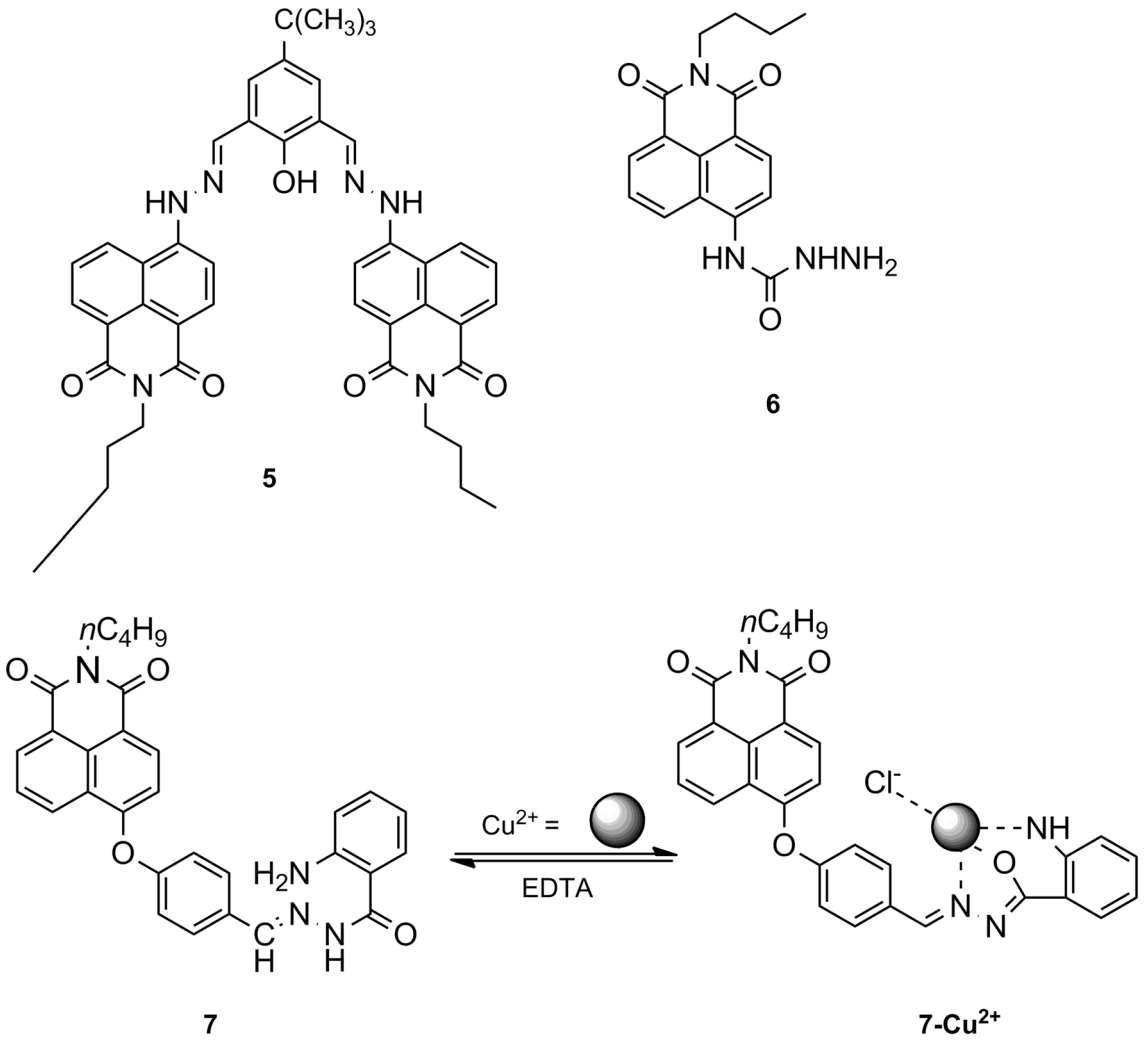

Fig. 6 Structures of **5** and **6** and structure of **7** with its reversible binding mechanism with Cu^{2+}

Hu and co-workers described a semicarbazide-based naphthalimide, **6**, as a colourimetric, fluorescent chemosensor for Cu^{2+} monitoring (Fig. 6) (Hu et al. 2015). In the presence of Cu^{2+} in buffer water/acetonitrile (80:20, v/v; pH 7.4), the compound underwent a significant enhancement in its fluorescence intensity. Importantly, **6** displayed high sensitivity and selectivity for Cu^{2+} over other tested alkali, alkaline-earth metals, and transition metal ions. The sensing of Cu^{2+} with **6** worked best within the linear range of 1.0×10^{-7}–100.0×10^{-7} mol L^{-1} ($R^2 = 0.9983$). The calculated detection limit was down to the level of 5.2×10^{-8} mol L^{-1}.

Yu's group constructed a simple 'off–on' fluorescent chemosensor **7** that bears the naphthalimide group (Yu et al. 2014b) with a detection limit and an association constant of 0.025 and 3.0×10^{-4} μM, respectively. **7** was effective for the detection of Cu^{2+} ion in ethanol–water solution (3:2, v/v, 50 mm HEPES, pH 7.4), amidst other tested metal ions and anions. **7** (Fig. 6) showed large fluorescence enhancement with Cu^{2+} ion, with linearity in the 0.05–1.5 μM range ($R = 0.999$). Following these results, the practicality of the chemosensor for real-time monitoring of Cu^{2+} was demonstrated by its potency to track Cu^{2+} ion in real water samples.

Chen et al. concerted their efforts to develop the naphthalimide derivative **8** that serves as a fluorescent chemosensor for Cu^{2+} detection (Chen et al. 2013b). In the presence of Cu^{2+} in acetonitrile–water (70:30, v/v) buffer solution of 3-(N-morpholino) propane sulfonic acid (MOPS, 10 mM, pH = 7.0), the fluorescence intensity of **8** was escalated (Fig. 7) in the order of a 4.5-fold enhancement. The linear detection range of **8** with Cu^{2+} lied between 4 μM to 7 μM with a detection limit of 0.15 μM calculated.

Lan and his team members intelligently designed two structurally similar fluorescent 'turn-on' naphthalimide-appended chemosensors for quantitative detection of Cu^{2+} among other metal ions, viz. K^+, Ag^+, Ca^{2+}, Mg^{2+}, Zn^{2+}, Pb^{2+}, Ni^{2+}, Mn^{2+}, Co^{2+}, Cd^{2+}, Hg^{2+}, Fe^{2+}, Fe^{3+} and Cr^{3+} (Fig. 7) (Lan et al. 2012). Upon Cu^{2+} chelation in acetonitrile solution, the fluorescence intensities of chemosensors **9** and **10** experienced tremendous uplift. The two-step binding mode of **9** with Cu^{2+} ion established the stoichiometric ratio of the chemosensor and analyte ion to be 1:1 and 1:2, which was further supported by ESI–MS results. The stability constants of **9** and **10** were obtained as 4.35×10^5 and 8.13×10^4, respectively. Desirably, Cu^{2+} monitoring by **9** and **10** was demonstrated to be reversible.

Georgiev and his lab members reported the design and synthesis of the blue-emitting, photostable, photoinduced electron transfer (PET) 1, 8-naphthalimide-based chemosensor **11** (Georgiev and Bojinov 2012). The group found that **11** (Fig. 8) switched between ''off'' and ''on'' states in the pH range of 9–6. So as to observe the discriminatory ability of the chemosensor, the team examined the fluorescence property of **11** in DMF solution using an array of various metal ions. A sharp fluorescence enhancement was observed upon Cu^{2+} addition (the fluorescence enhancement was of the order of 18.6) in the presence of metal ions (Cu^{2+}, Pb^{2+}, Cd^{2+}, Ni^{2+}, Co^{2+}, Fe^{3+} and Zn^{2+}) and protons. Other co-existing metal ions and proton induced no notable change on the fluorescence intensity of **11**.

Yu et al. reported the novel 'off–on' type fluorescent chemosensor **12** that anchors both naphthalimide and rhodamine B units, as an effective chemosensor capable of distinguishing Cu^{2+} ion in an assembly of other cations (Yu et al. 2011). In ethanol–water (1:9, v: v, 50 mM HEPES, pH 7.0) solution, there was an increase in the fluorescence intensity of **12** upon treatment with 10 equiv. of Cu^{2+}. The calculated detection limit was suitably low down to the level of 0.18 μM.

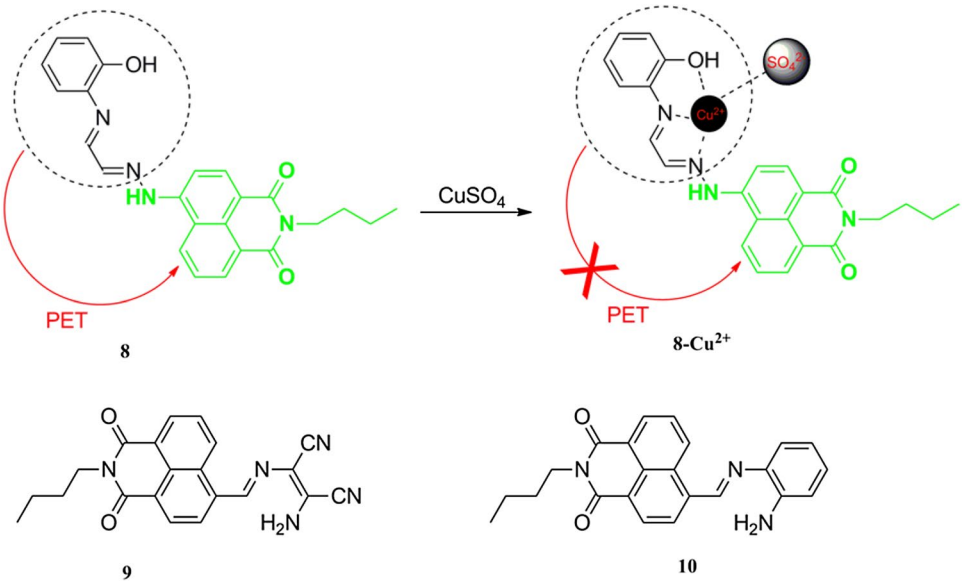

Fig. 7 Structure of **8** displaying its complexation mode with Cu^{2+} (up) and structures of **9** and **10** (down)

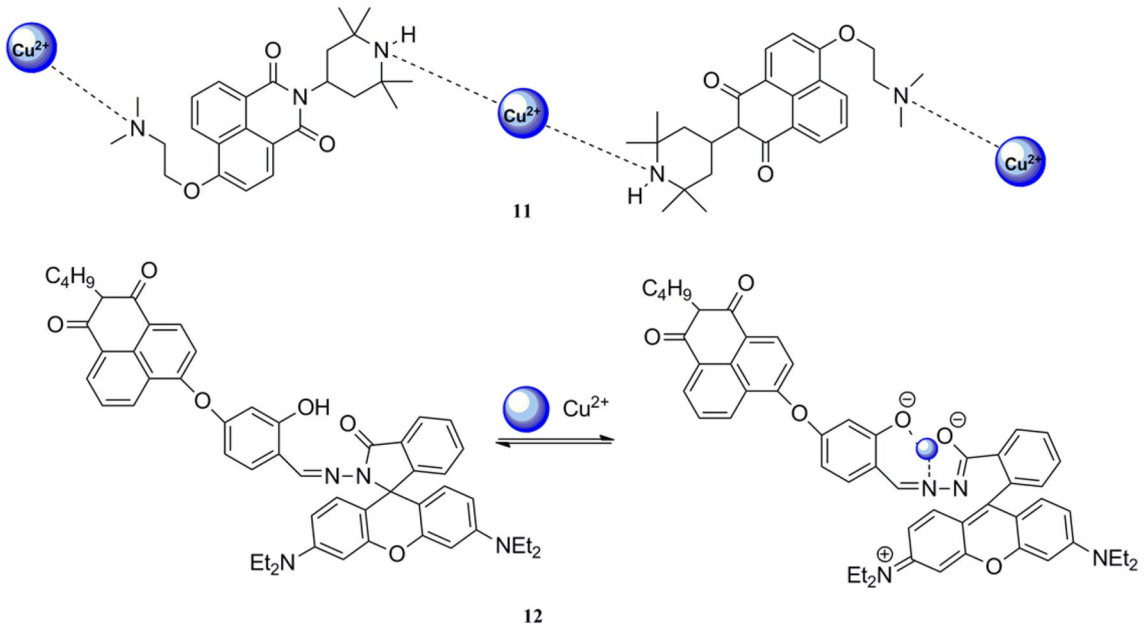

Fig. 8 Proposed modes of complexation of **11** and **12** towards Cu^{2+}

Study of the binding ratio of **12** and Cu^{2+} revealed a 1:1 stoichiometry mode (Fig. 8). The compound was reversible in its sensing nature and was able to visualise Cu^{2+} in living cells in biological systems.

Xu et al. in 2010 reported the fluorescent chemosensor **13** that bears a naphthalimide unit connected to a piperazine ring. The reported compound could sensitively and selectively detect Cu^{2+} amongst other investigated cations (Fig. 9) (Xu et al. 2010d). Free **13** displayed a dynamic excimer emission in polar solvents, which results from the naphthalimide dimer formed in the excited state. Meanwhile, complex **13**-Cu^{2+} exhibited static excimer emission which arises from naphthalimide dimer in the ground state. Job's plot furnished a 1:2 complexation ratio of **13** and Cu^{2+} in **13**-Cu^{2+}. A dramatic increase in the fluorescence intensity of **13** towards Cu^{2+} in aqueous solutions (CH_3CN:HEPES = 1:1, v/v) was observed, but not in the case of other metal ions. The calculated dissociation constant (K_d) of **13** with Cu^{2+} was 3.4×10^{-4} M.

Xu et al. in 2010 again developed two 4, 5-disubstituted-1, 8-naphthalimide derivatives, **14** and **15**, which shows a good response for Cu^{2+} monitoring (Fig. 9) (Xu et al. 2010b). Compound **14** behaved as a fluorescent chemosensor while compound **15** acts as a colourimetric chemosensor. A significant enhancement in the fluorescence intensity of **14** at 478 nm in 100% aqueous solution took place upon the addition of Cu^{2+}, well distinct from that of the fluorescent emission of 1**4** centred at 534 nm. The results that proceeded from the spectroscopic investigations showed that compound **15** could sense Cu^{2+} ion through massive quenching of its fluorescence intensity and concomitant colour change from primrose yellow to pink.

Hg^{+} ion-selective chemosensors

The analytical capacity of the 1, 8-naphthalimide-based compound **16** as a fluorescent chemosensor for Hg^{2+} monitoring was appraised by La's group. The group further demonstrated that the compound also possessed colourimetric sensing properties towards CN^{-} and F^{-}, acting as both cationic- and anionic-specific multianalyte chemosensor (Fig. 10) (La et al. 2016). Results revealed that the compound experienced an amplification of its fluorescence signal intensity upon the addition of Hg^{2+} while other investigated anions and cations left only rather benign changes in the fluorescence signal intensity of the chemosensor. There was linearity of response of the chemosensor in its monitoring of Hg^{2+}, with the detection limit and association constant determined to be 2.4×10^{-7} and 4.12×10^{5} M, respectively. Job's plot analysis gave a binding ratio of 1:1, which was further evidenced by ^{1}H NMR results.

Li's research group devised two naphthalimide-appended fluorescent chemosensors, **17** and **18** (Fig. 10) for Hg^{2+} detection (Li et al. 2016a). Compounds **17** and **18** were capable of Hg^{2+} ion detection over a wide pH span of 7.0–10.0. In 10 μM solution of **17** in phosphate buffer (pH 7.5) containing various metal ions, only Hg^{2+} could suppress the fluorescence intensity of **17** by about 90%; meanwhile, other competitive cations collectively impressed only mild effects on the fluorescence intensity of **17**. Compound **18** showed a

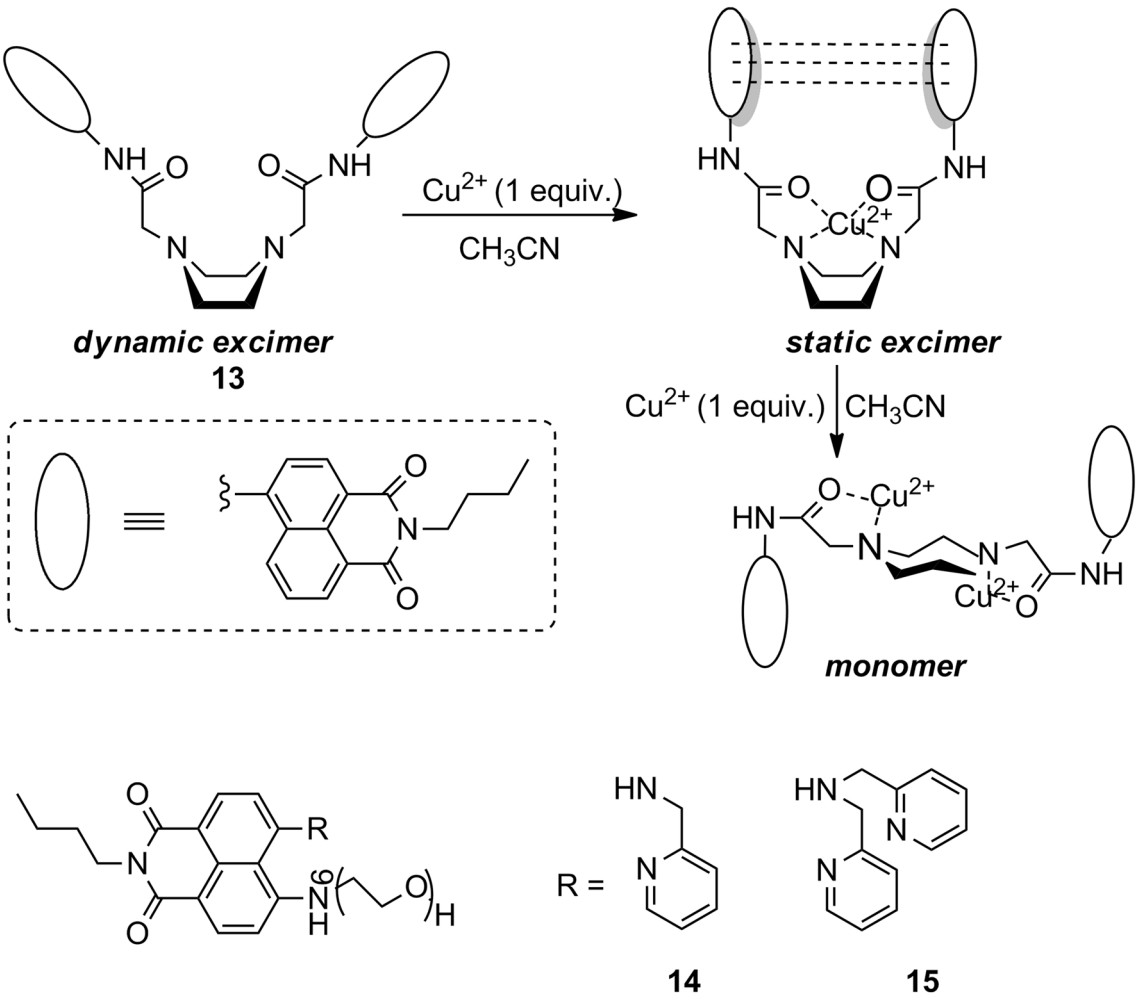

Fig. 9 Proposed sequential binding mode of **13** with Cu^{2+} (up) and structures of **14** and **15** (down)

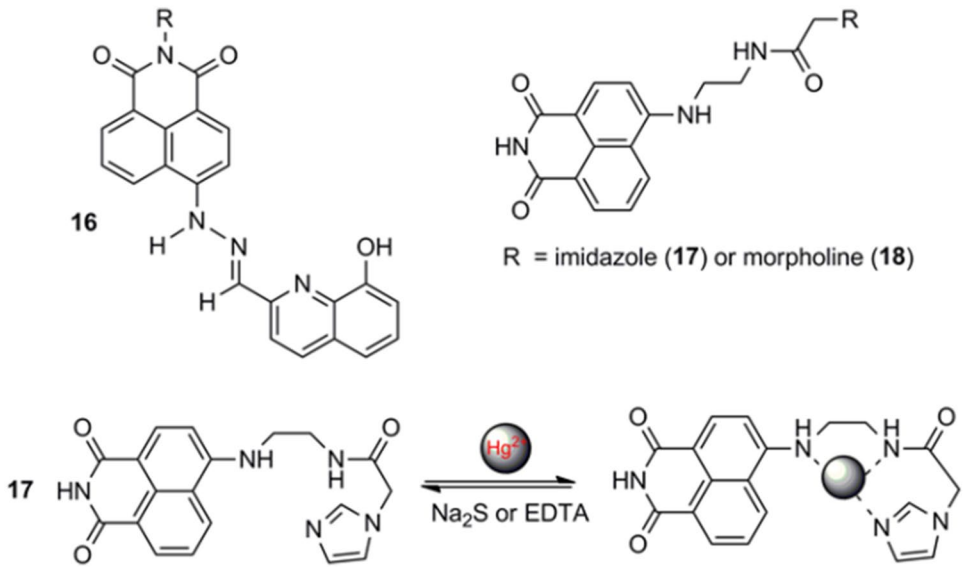

Fig. 10 Structure of **16** (top-left), structures of **17** and **18** (top-right) and binding mechanism of **17** with Hg^{2+} showing its reversible nature upon the addition of EDTA (down)

similar observation as with compound **17**. The linear range of detection of Hg^{2+} by **17** was between 2 and 10 µM, and the detection limits of **17** and **18** for Hg^{2+} tracking were 2.1 and 3.1 µM, respectively.

Vonlanthen and his team members explored the Hg^{2+}-sensing properties of the PET naphthalimide-based chemosensor **19** (Vonlanthen et al. 2014). No fluorescence enlargement was observed at pH 5.5 or lower, but there was noticed significant fluorescence enhancement towards Hg^{2+} in 9:1 H_2O/CH_3OH. Job's plot established a 1:1 stoichiometric ratio between chemosensor **19** and Hg^{2+} ion (Fig. 11). It is only fair to note that the compound was successfully applied for Hg^{2+} imaging in living mammalian cells.

Un and co-workers brought into being a simple but effective fluorescent chemosensor that utilises the 1, 8-naphthalimide unit for a 'turn on' detection of Hg^{2+} ion (Fig. 12) (Un et al. 2014a). Titration of aqueous solution (THF–H_2O, 1:1, pH 7.4, 10 mM Tris–HCl) of this compound in co-existence with several other metal ions induced a notable enhancement of fluorescence towards Hg^{2+} only. The fluorescence detection was linear within the range of 1–30 µM. The corresponding detection limit and association constant were estimated as 6.28×10^{-8} M and 5.4×10^{4} M^{-1}, respectively. From real-world application standpoint, the fluorescence imaging of Hg^{2+} in living cells by **20** was successfully demonstrated.

Moon and co-workers introduced a thionaphthalimide-based chemosensor **21** and its two monothio derivatives, **22** and **23** (Fig. 12), responsive for Hg^{2+} monitoring via an 'off–on' modality (Moon et al. 2013). Upon the addition of Hg^{2+} to chemosensor **21** in 30% aqueous CH_3CN solutions, there was enlargement of the fluorescence intensity of **21** at

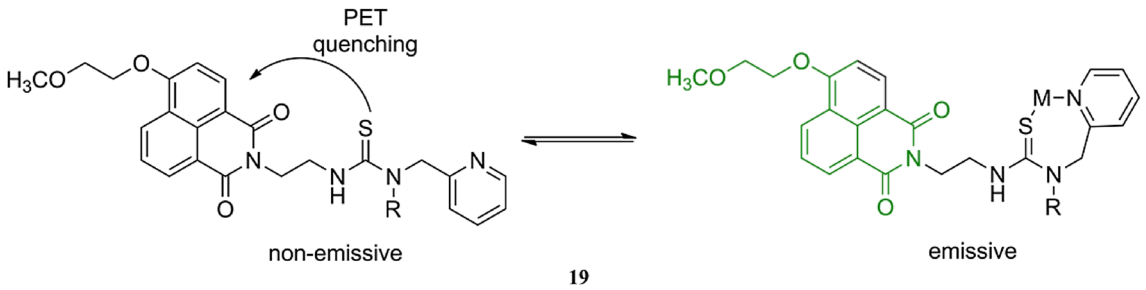

Fig. 11 Structure of **19** showing PET mechanism

Fig. 12 Structures of **20–23**

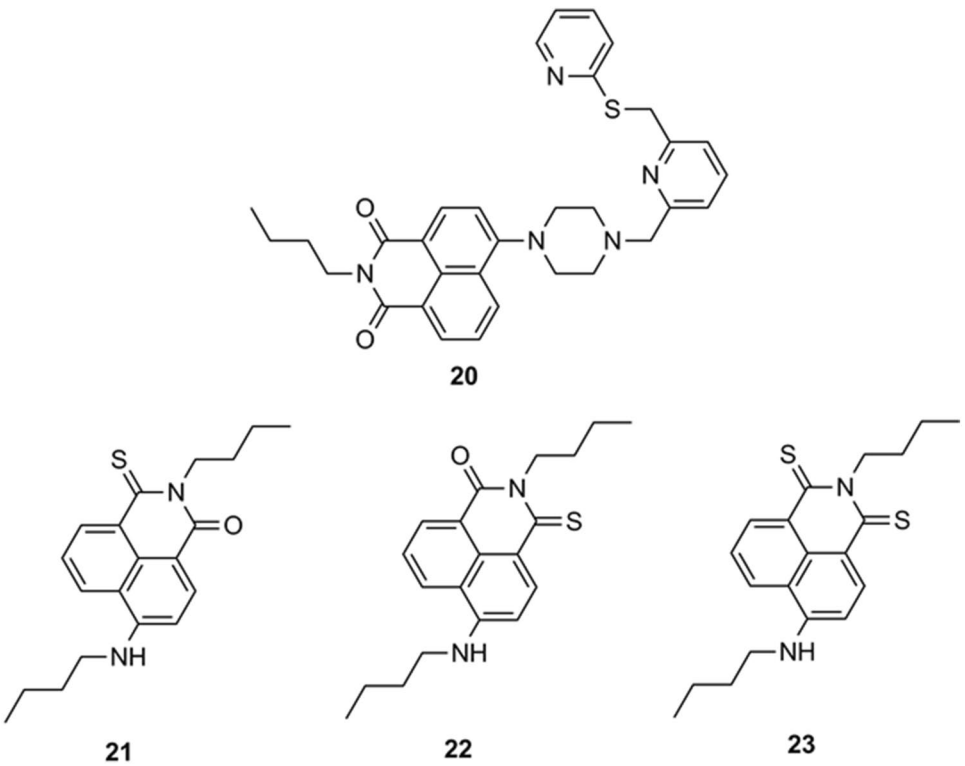

537 nm. Meanwhile, other investigated background metal ions left no tremendous effect on the fluorescence intensities of chemosensors **22** and **23**. The estimated detection limit of the reported **21** for the sensing of Hg^{2+} ions was 2.7 μM.

The laboratory of Zhang et al. reported a new fluorescent molecule **24** (Fig. 13), for the recognition of Hg^{2+} among several other metal ions, including Na^{+}, K^{+}, Ca^{2+}, Mg^{2+}, Cu^{2+}, Zn^{2+}, Cr^{2+}, Pb^{2+}, Ni^{2+}, Fe^{2+}, Mn^{2+}, Co^{2+}, and Cd^{2+} (Zhang et al. 2013a). Successive addition of Hg^{2+} in EtOH/H_2O (1/2, v/v) to solution of the chemosensor led to sharp increment in the fluorescence intensity of **24** while no obvious change was observed for other tested cations. Their findings indicated the existence of a 1:1 binding stoichiometry between Hg^{2+} and **24** in complex **24**-Hg^{2+} (from Job's plot analysis).

Li et al. made a report of the PET naphthalimide-based chemosensor **25** that anchors a hydrophilic hexanoic acid group, for the recognition of Hg^{2+} (Fig. 13) (Li et al. 2012a). Experimental data showed that the compound was most suitable for Hg^{2+} tracking within a linear range of 2.57×10^{-7}–9.27×10^{-5} M. Job's plot deciphered a 1:1 binding mode of chemosensor **25** and Hg^{2+} with a detection limit of 4.93×10^{-8} M estimated. In Tris–HNO_3 buffer solution of pH 7.0, the chemosensor displayed great enhancement in its fluorescence intensity upon Hg^{2+} addition in coexistence with other metal ions. The response time of Hg^{2+} detection by **25** was less than 1 min. **25** was reversible in its sensing mechanism. Noteworthy is that the chemosensor was successfully applied for Hg^{2+} determination in hair samples.

Yang et al. described a new PET fluorescent chemosensor that incorporates the naphthalimide structure as fluorophore unit (Fig. 13) (Yang et al. 2012). Compound **26** retained excellent affinity for Hg^{2+} in the presence of a family of environmentally and biologically significant metal ions. In methanol–water (1:9, v/v) solution, there was enlargement of the fluorescence intensity of **26** (about fourfold increment) upon the gradual addition of Hg^{2+}. The response of chemosensor **26** towards Hg^{2+} was linear within the concentration range of 0–10 μM. The detection limit and association constant were estimated as 63 nM and 1.11×10^{5} M^{-1}, respectively. Of note is that the chemosensor can reversibly respond to Hg^{2+} detection.

Li and his teammates prepared the 'turn-on' fluorescent chemosensor **27** effective for Hg^{2+} tracking amidst a host of other cations (Li et al. 2012b). The addition of 1.0 equivalent of Hg^{2+} to THF solution of **27** led to a 110-fold increment of the fluorescence intensity, in contrast to other examined metal ions that did not modulate the fluorescence intensity of **27**. The compound functioned best for Hg^{2+} monitoring within the pH range of 5.0–9.0. The fluorescence titrations of **27** with Hg^{2+} were further conducted under optimised conditions (acetone/water = 1/1, v/v, pH = 7.0), with a 100-fold fluorescence enhancement observed. Further experiments established that chemosensor **27** (Fig. 14) was outstanding for imaging HL cells by a confocal laser scanning microscopy.

Liu and co-workers developed a new chemosensor **28**, which contains both rhodamine B and naphthalimide units (Liu et al. 2012). The compound detected Hg^{2+} in a wide pH range of 5.7–11.0. Upon the addition of 1 equiv. of Hg^{2+}, weak fluorescence emission was observed at 585 nm in 2:1 (v/v) MeOH/water solution (10 mM Tris–HCl, pH 7.0). The compound (Fig. 14) worked optimally within the linear

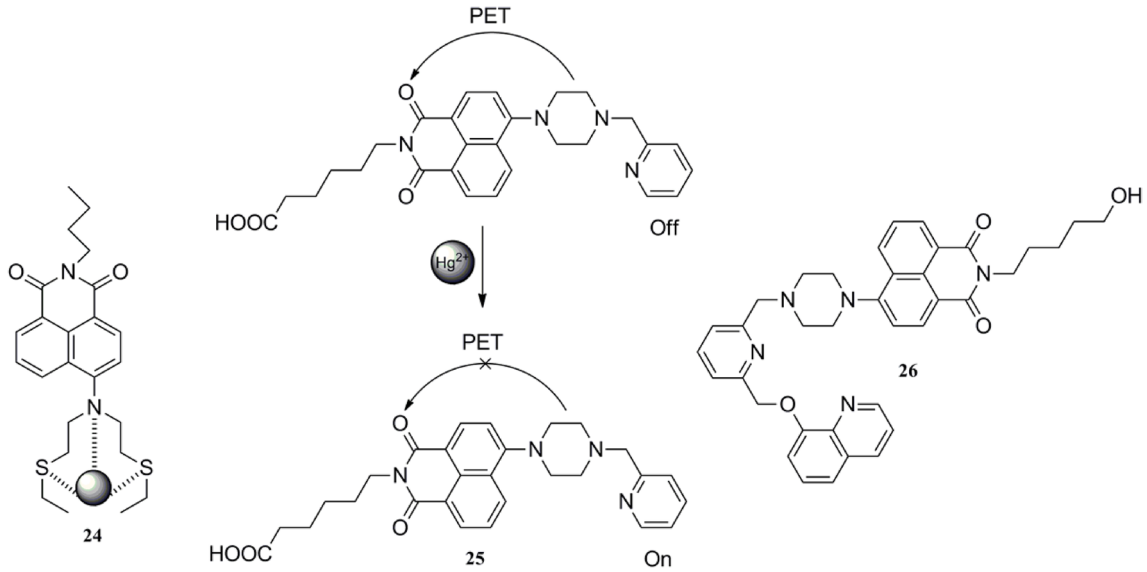

Fig. 13 Structure of **24** (left), binding mechanism of **25** with Hg^{2+} (middle) and structure of **26** (right)

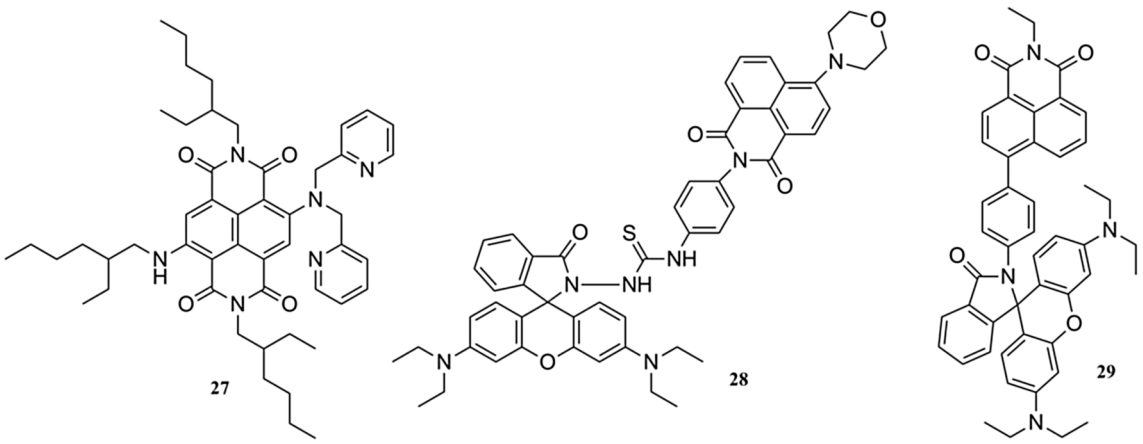

Fig. 14 Structures of **27**–**29**

range of 2–10 mM. Job's plot analysis yielded a maximum at 0.5 mol fraction, implying the formation of a 1:1 complex of **28** with Hg^{2+}.

Kumar et al. obtained the 1, 8-naphthalimide-appended fluorescent chemosensor **29** (Fig. 14) (Kumar et al. 2011) whose binding behaviour and fluorescence response were studied towards different metal ions in mixed aqueous media (THF/H_2O; 9.5:0.5). Results showed that the addition of the investigated cations (except for Hg^{2+}) did not give rise to any significant change in the fluorescence intensity of **29**. This clearly demonstrates that the compound has excellent affinity for Hg^{2+} over these ions. The detection limit of **29** for Hg^{2+} was calculated to be 2×10^{-6} mol L^{-1}. Job's plot method of continuous variation gave a stoichiometric ratio of 1:1. The binding behaviour of Hg^{2+} ion to chemosensor **29** was analytically reversible. The potential biological application of the chemosensor was assessed for Hg^{2+} monitoring ion in prostate cancer (PC3) cell lines.

Cr^{3+}-selective chemosensors

Yu et al. generated the 1, 8-naphthalimide-based chemosensor **30** for singular and reversible detection of Cr^{3+} (Fig. 15) (Yu et al. 2016). Fluorescence titration experimental results revealed gradual addition of Cr^{3+} to solution of the chemosensor (1.0×10^{-5} M, water/ethanol = 6:4, v/v) in the presence of the other cations amplified the fluorescence intensity of **30**. In contrast, the addition of other cations did not modulate any significant change in the fluorescence intensity of **30**. Cr^{3+} sensing with compound **30** was desirably linear in the range 0–5.5×10^{-5}. The calculated detection limit was found to be as low as 0.60 ppm. Above all, the ability of the chemosensor to monitor biological samples of HeLa cells was successfully demonstrated.

Xue et al. reported the use of the colourimetric, fluorescent 1, 8-naphthalimide-based chemosensor **31** that simultaneously bears rhodamine B and diarylethene units (Xue et al. 2015). The chemosensor upheld strict Cr^{3+} monitoring ability. Addition of various metal ions (10 equiv.) to the chemosensor in acetonitrile (2.0×10^{-5} mol L^{-1}) solution led to insignificant modulation of the initially weak fluorescence intensity of **31** at 370 nm, except in the case of Cr^{3+}. The mentioned compound **31** possessed vibrant regeneration property as evidenced by its reversibility nature in the detection of Cr^{3+}, whereby free **31** was unbound from complex **31**-Cr^{3+} (Fig. 15).

Wu and co-workers published their development of the PET fluorescent chemosensor **32** that anchors the naphthalimide architecture (Fig. 15) (Wu et al. 2014). The designated compound was highly sensitive and selective for Cr^{3+} tracking amidst other investigated metal ions in THF/H_2O solution (85/15, v/v) through a fluorescence 'turn on' mode. A 1:1 binding mode between **32** and Cr^{3+} was furnished by MALDI-TOF–MS analysis. The fluorescence detection response of Cr^{3+} determination by **32** was desirably linear in the 20–120 μM range. Meanwhile, the detection limit and association constant were determined to be 0.20 μM and 2.4×10^4 M^{-1}, respectively.

Fe^{3+} ion-selective chemosensors

In the attempt to construct chemosensors that could detect Fe^{3+} effectively, Li and co-workers designed the fluorescence enhancement chemosensor **33** (Fig. 16) that bears coumarin and naphthalimide (Li et al. 2014). In THF-H_2O (v/v, 1:1) solution, the chemosensor exerted a high selectivity for Fe^{3+} over other investigated metal ions with a massive fluorescence intensity enlargement at 456 nm. Job's plot gave the binding ratio of compound **33** and Fe^{3+} in the **33**-Fe^{3+} complex as 1:1 (Fig. 16). The association constant and detection limit were calculated to be $(2.589 \pm 0.206) \times 10^3$ M^{-1} and 0.388 mM, respectively.

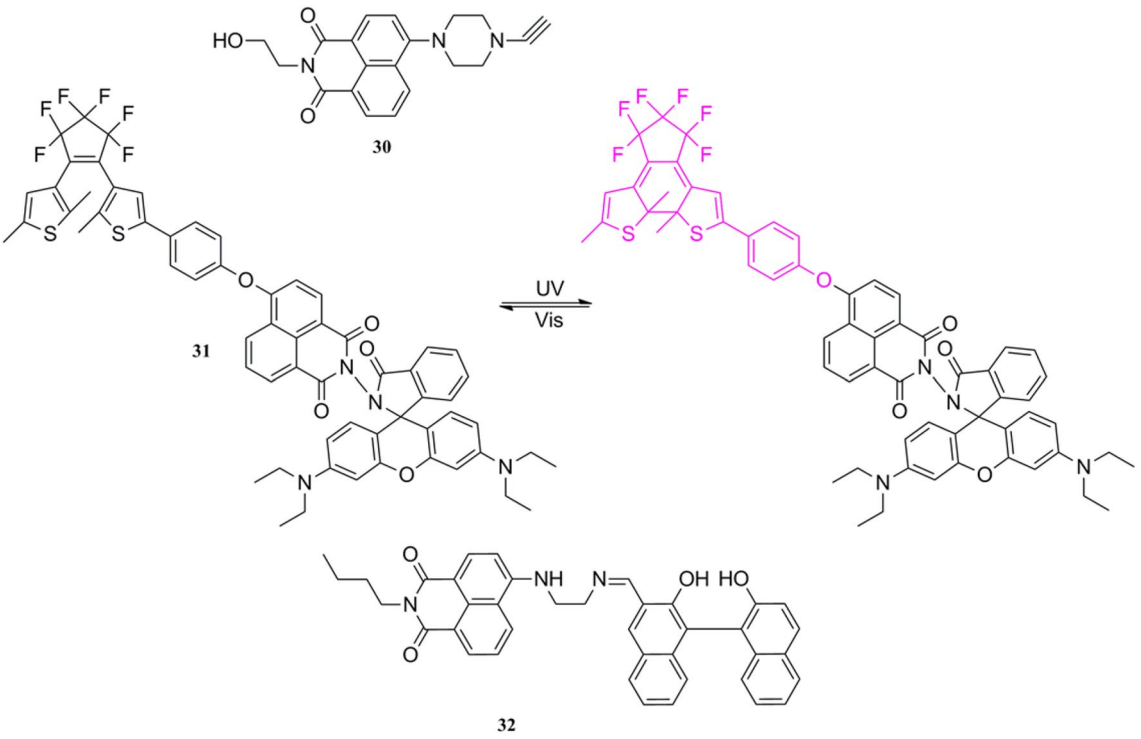

Fig. 15 Structure of **32** (up), illustration of the photochromism of **31** (middle) and structure of **32** (down)

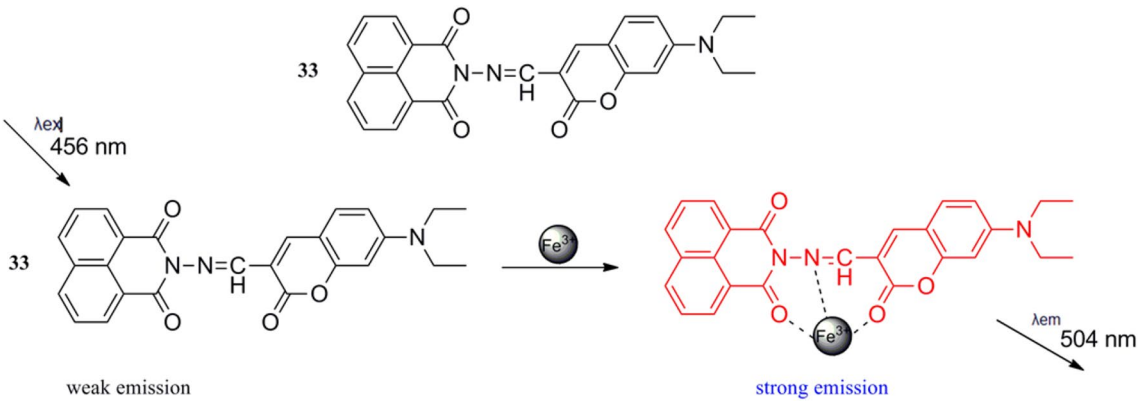

Fig. 16 Structure of **33** (up) and schematic illustration of its binding mechanism with Fe^{3+} (down)

Chereddy and co-workers introduced the PET-operated naphthalimide-based fluorescent chemosensor **34** capable of singular detection of Fe^{3+} in coexistence with other cations (Fig. 17) (Chereddy et al. 2014). While the addition of Fe^{3+} amplified the fluorescence intensity of **34** in Tris–HCl–CH_3CN solution (v/v, 1:1; 0.01 M Tris–HCl–CH_3CN; pH 7.4), the addition of other rival cations impacted collective insignificant effect on the fluorescence intensity of **34**. The binding constant was calculated as 1.04×10^5 M^{-1} while the detection limit was determined to be 3.0×10^{-8} M. Ultimately, the reported compound **34** was reversible in its Fe^{3+} detection mechanism.

Yang and teammates showed that the fluorescent chemosensor **35** that bears three 1, 8-naphthalimide units in its structure could rapidly monitor Fe^{3+} (Yang et al. 2013). The addition of various competitive metal ions to **35** in DMF/H_2O (v/v, 4:1 and 2:3) did not affect the fluorescence intensity of **35** much, except for Fe^{3+} that impinged an escalation on the fluorescence intensity of the compound. Based on the fluorescence titration, the calculated detection limit and binding constant were 4.69×10^{-7} M and $2.406 \times$ M^{-1},

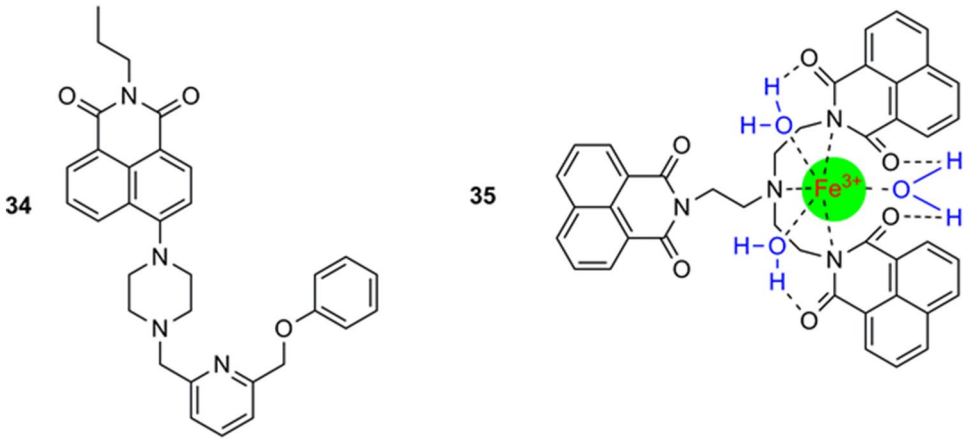

Fig. 17 Structure of **34** (left) and structure of **35**-Fe^{3+} complex (right)

respectively. The result obtained from Job plot indicated a 1:1 binding of **35** and Fe^{3+} in the complex **35**-Fe^{3+} (Fig. 17).

Xu's research group generated the optode membrane kind of a naphthalimide derivative **36** having terminal double bond (Fig. 18) (Xu et al. 2013). The reported compound was highly sensitive and selective for Fe^{3+} sensing amongst other tested cations. The incremental addition of Fe^{3+} to **36** in 0.05 mol/L Tris/HCl (pH 6.02) lowered the fluorescence intensity of the chemosensor rapidly. Strikingly, **36** showed excellent sensing properties as validated by its wide linear tracking range of 1.0×10^{-5}–1.0×10^{-3} M and low detection limit of 4.5×10^{-6} M. The experimental optimum working pH range was between 5.00 and 8.00. The developed compound was reversible in its sensing mechanism and above all, it was successful in Fe^{3+} monitoring in pharmaceutical preparation samples.

Staneva and his peers proved that the poly(propylene amine) dendrimer **37** (Fig. 19) that incorporates four 4-(*N*, *N*-dimethylaminoethyloxy)-1, 8-naphthalimide units, could be effective as a chemosensor for Fe^{3+} detection in acetonitrile solution (Staneva et al. 2012). It was reported that the compound, upon Fe^{3+} addition, exhibited large fluorescent amplification (of the order of 44.95). Meanwhile, its fluorescence intensity remained unchanged upon the addition of other metal ions under similar testing condition. Furthermore, good linearity of response of Fe^{3+} monitoring by **37** was observed within the concentration range of 2×10^{-7}–4.10^{-6} mol L^{-1}. Finally, the detection limit of **37** with Fe^{3+} was estimated as 2×10^{-7} mol L^{-1}.

Zn^{2+} ion-selective chemosensors

The fluorescent chemosensor **38** that operates through a dual PET-ICT mechanism (Fig. 20) (Wei et al. 2015) was developed by Wei and co-workers in 2015. The initially weak fluorescence of this compound, positioned at the emission wavelength of 465 nm underwent amplification upon the incremental addition of Zn^{2+} in neutral aqueous solution (10 mM Tris–HCl buffer, pH 7.2, containing 1% CH_3CN), while the addition of other rival ions left no significant change in the fluorescence of the compound. The linearity of detection of Zn^{2+} by the chemosensor was demonstrated to be in the range 0–120.0 μM. The calculated detection limit and association constant were 7.2×10^{-9} M and 6.27×10^{4} M^{-1}, respectively. Consequently, the developed compound was utilised to image Zn^{2+} in living HeLa cells.

Liu and his research group members developed the fluorescent chemosensor **39**, which contains 4-amino-1,

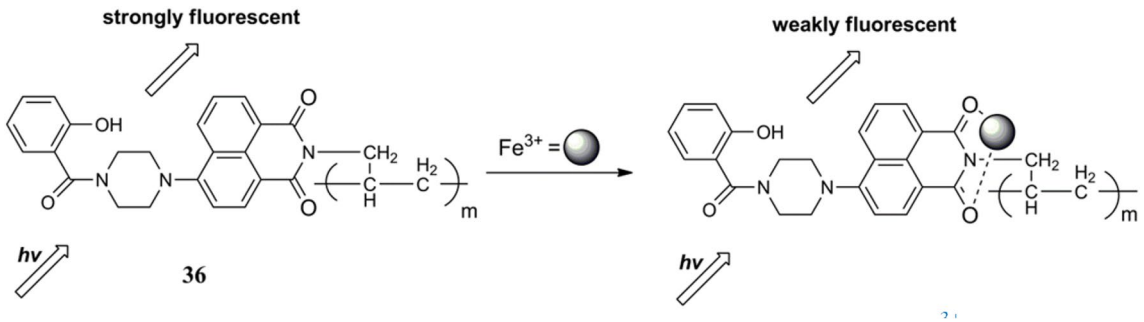

Fig. 18 Structure of **36** showing its detection mechanism of Fe^{3+}

Fig. 19 Structure of **37**

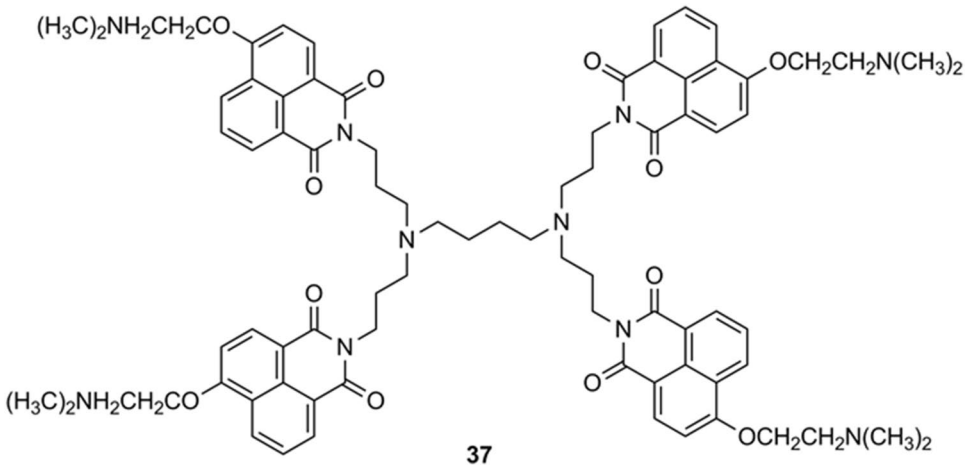

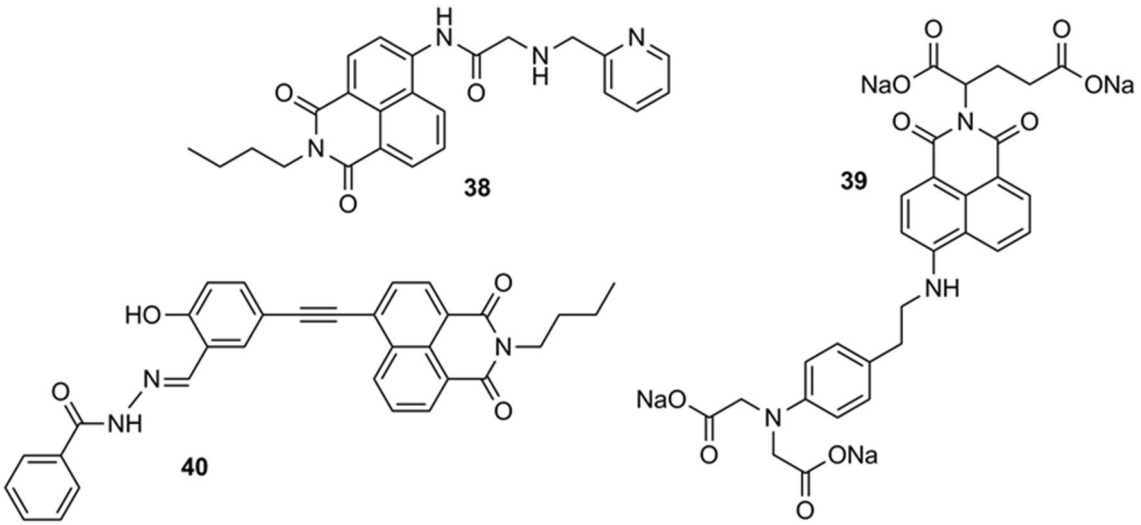

Fig. 20 Structures of chemosensors **38**–**40**

8-naphthalimide as fluorophore and iminodiacetic acid as receptor (Fig. 20) (Liu et al. 2014). The gradual addition of Zn^{2+} to solution of **39** in 20 mM HEPES buffer (pH 7.4) caused an increment in the fluorescence emission intensity of the chemosensor (in the order of a 50-fold increase). Compound **39** was successfully applied to image Zn^{2+} in living cells. However, the addition of other metal ions imposed no monumental fluorescence change. Chemosensor **39**, whose calculated dissociation constant reached the level of 2.4×10^{-5} M, was successfully applied to bioimage Zn^{2+} in living cells.

The 1, 8-naphthalimide derivative that functions as a turn-on fluorescent chemosensor **40** for Zn^{2+} detection was prepared by Zhao's research group (Zhao et al. 2013). In aqueous medium (CH_3CN/HEPES, v/v = 6:4, pH 7.4), the ligand interacted with Zn^{2+} with notable fluorescence increment of about 13-fold increase ensuing from the process, whereas other cations did not significantly alter the fluorescence of the chemosensor. The values of the detection limit and association constant of **40** towards Zn^{2+} are 1.03×10^6 M and 3.02×10^3 M^{-1}, respectively. The reported compound (Fig. 20) was successfully applied to image Zn^{2+} in A549, BEAS-2B, CHO, HeLa, and HepG2 cells.

Hanaoka et al. fabricated the water-soluble, fluorescence 'off–on' 4-amino-1, 8-naphthalimide-based chemosensor **41** that utilises ICT mechanism in its detection mode of Zn^{2+} (Fig. 21) (Hanaoka et al. 2010). In HEPES buffer (100 mM, pH 7.4), the compound displayed high affinity for Zn^{2+} (in co-existence with other cations) with a significant signal amplification of 21.7-fold. The apparent dissociation constant of **41** for Zn^{2+} detection was estimated as 1.1 nM. Desirably, the chemosensor was effective for Zn^{2+} bioimaging in cultured HeLa cells in 10 μM HBSS buffer.

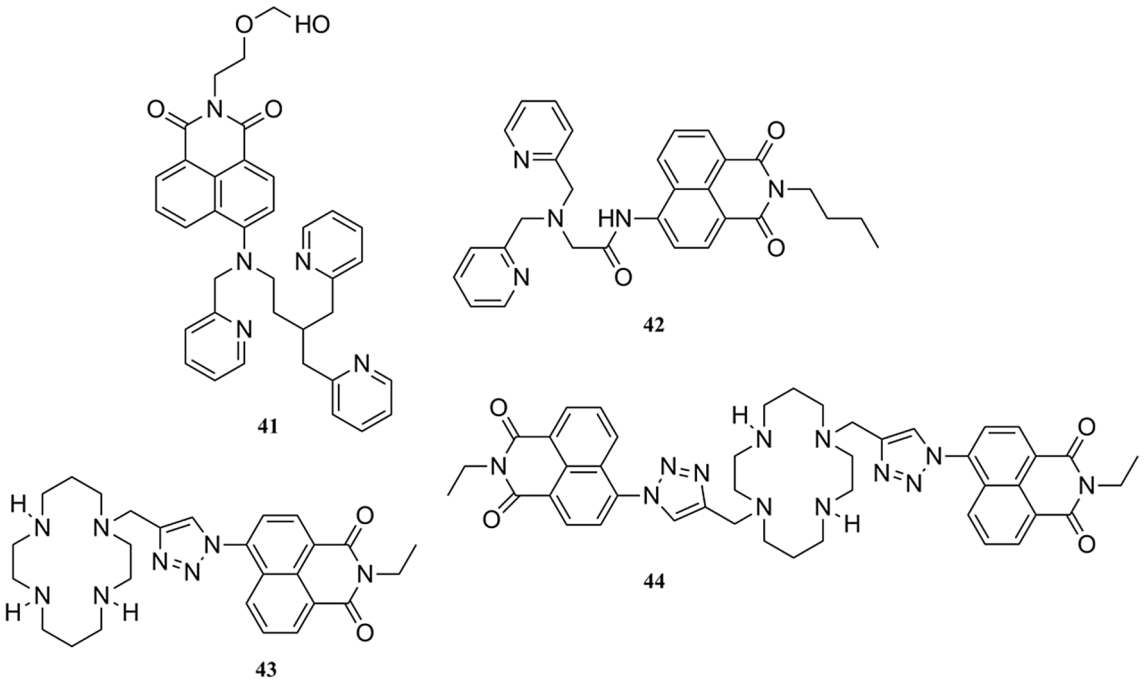

Fig. 21 Structures of **41**–**44**

Xu and co-workers described the fluorescence 'off–on' PET chemosensor **42** whose structure comprises 1, 8-naphthalimide unit as fluorophore and di-2-picolylamine unit as receptor (Fig. 21) (Xu et al. 2010a). In CH_3CN-HEPES (v/v, 1:9, HEPES 0.5 M, pH = 7.4), the chemosensor participated in fluorescence enhancement process upon contact with Zn^{2+} among other metal ions of interest. The remaining cations induced no dramatic effect on the fluorescence spectra of **42**. A 1:1 binding mode of compound **42** with Zn^{2+} was given.

Tamanini et al. showed that variant compounds of the same parental block could behave as homogeneous and heterogeneous chemosensors for Zn^{2+} detection. The reported PET compounds **43** and **44** (Fig. 21) (Tamanini et al. 2010) are typical examples of such compounds. Compounds **43** and **44** exhibited fluorescence enhancement towards Zn^{2+}; the latter compound displays twofold fluorescence property than the former. In H_2O/CH_3CN (7:3) buffer solution (50 mM HEPES buffer; pH 7), large fluorescence increment in the fluorescence signal of **44** (10 μM) was observed upon the addition of 1 equiv. of Zn^{2+} (a 12.7-fold amplification) amidst other divalent cations. The fluorescence of **44** was slightly suppressed by Cu^{2+} and Hg^{2+}. The calculated dissociation constant of **44** was 10^7 M^{-1}. Ligands **43** and **44** were employed for the fabrication of nanostructured zinc chemosensors via the sol–gel process.

Ag^+ ion-selective chemosensors

The novel mono- and di-substituted *N*–n-butyl-1, 8-naphthalimide derivative **45**, efficient as a fluorescent chemosensor for Ag^+ tracking was reported by Fu et al. (Figure 22) (Fu et al. 2016). Results showed that the addition of foreign cations to **45** in ethanol–water solution (4:1, v/v, 10 mM HEPES buffer, pH = 7.06) did not result in any change in the fluorescence intensity of **45** except for Ag^+ that lowered the chemosensor's fluorescence intensity at the emission wavelength of 535 nm. Job's plot analysis indicated the formation of a 2:1 complex between **45** and Ag^{+}.

The lab of Zhou and co-workers made a breakthrough in the fabrication of the 4-amino-1, 8-naphthalimide-based compound **46**, which anchors Schiff base and vanillin units (Zhou et al. 2012). In its detection mode, compound **46** acted as a fluorescent chemosensor with strict singularity for Ag^+ over other various cations under the same experimental condition. The fluorescence intensity of **46** was dampened upon the incremental addition of Ag^+ at 682 nm. The estimated detection limit was low, down to the level of 3.0×10^{-6} mol L^{-1}. Job's method of continuous variation gave the binding ratio of **46** and Ag^+ in **46**-Ag^+ complex to be 2:1 (Fig. 22).

Xu and co-workers designed two structurally similar naphthalimide derivatives **47** and **48** (Fig. 22) as fluorescent chemosensors for Ag^+ monitoring (Xu et al. 2010e). In aqueous solution (CH_3CN: HEPES = 50:50, v/v; 0.5 M HEPES buffer

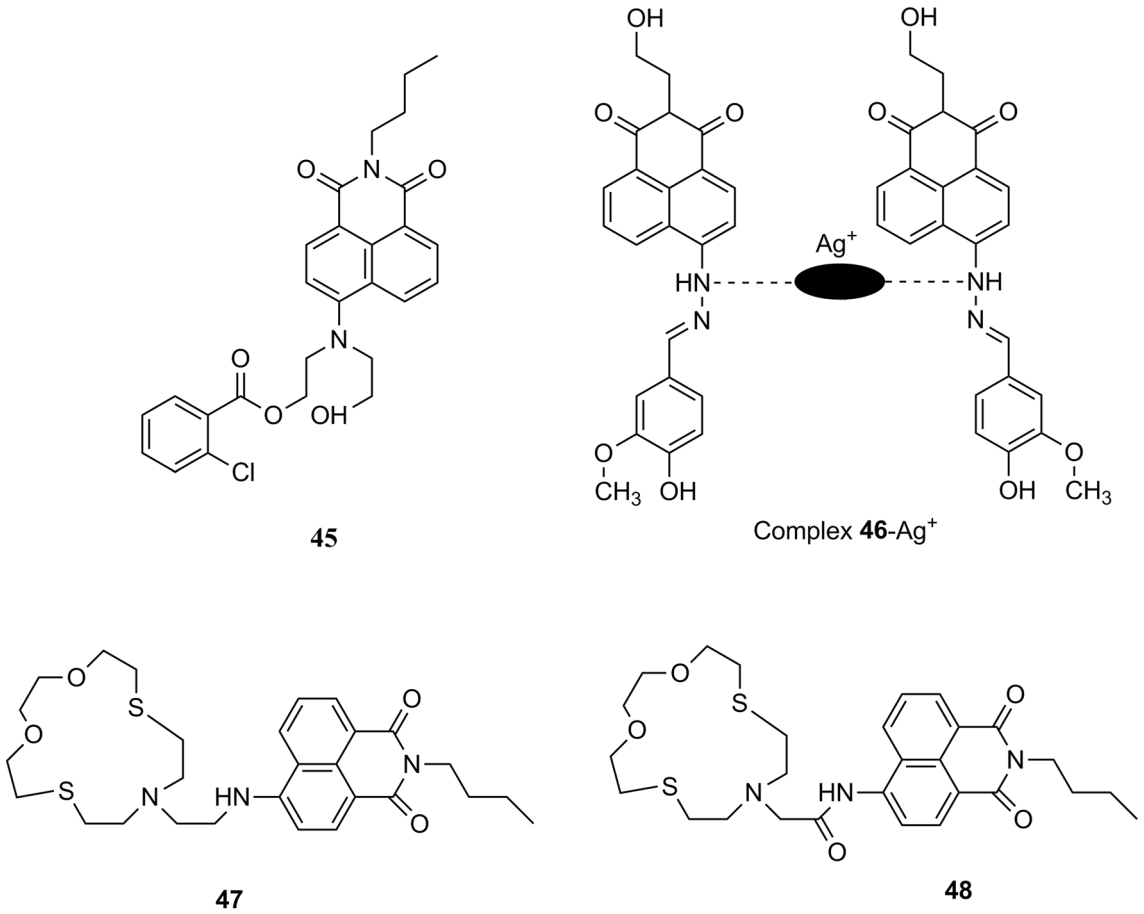

Fig. 22 Structures of **45**–**48**

at pH 7.4), compound **47** detects Ag^+ effectively with an approximate 14-time enhancement of its fluorescence. Large association constant of 1.24×10^5 M^{-1} was determined for **47** and low detection limit of 1.0×10^{-8} M was calculated for **48**. The reference compound **48**, devoid of carbonyl group, did not strongly bind with Ag^+ owing to that the carbonyl group between 1, 8-naphthalimide and [15]aneNO_2S_2 played an active role in the increment of the fluorescence intensity.

Pd^{2+}-selective chemosensors

Liu and teammates developed the novel water-soluble fluorescent chemosensor **49** (Fig. 23) for Pd^{2+} monitoring in phosphate-buffered saline (PBS) solution (10 μM, pH 7.4), which operated within the linear range of 0–6 μM ($R^2 = 0.995$) and with the low detection limit of 25 nM or 2.7 μg/L calculated (Liu et al. 2014). The incremental addition of 5.0 equiv. of 21 different metal ions to solution of compound **49** impressed a rather insignificant effect on the fluorescence intensity of **49**. Meanwhile, only Pd^{2+} left a massive increment (sevenfold) in the fluorescence intensity of **49**. The efficacy of the reported compound was delineated by its ability for the intracellular fluorescence imaging of Pd^{2+} in Hep G2 and HL60 living cells.

Wang et al. evaluated the sensing properties of the fluorescent chemosensor **50** towards Pd^{2+} (Fig. 23) (Wang et al. 2012). The optimal pH range for Pd^{2+} detection as revealed by experimental analysis was between 6 and 9. In phosphate-buffered saline (PBS) (10 mM, pH 7.4) solution, the designated compound only had affinity for Pd^{2+} amongst others metal ions (i.e. Ca^{2+}, Mg^{2+}, Zn^{2+}, Cd^{2+}, Ni^{2+}, Li^+, Mn^{2+}, Cu^{2+}, Na^+, K^+, Co^{2+}, Ag^+, Pb^{2+}, and Hg^{2+}) in coexistence under the same analytical condition. The fluorescence intensity of **50** was enlarged by Pd^{2+} in the order of 7.2-fold enlargement.

Jiang and his team members constructed the colourimetric, ratiometric fluorescent chemosensor **51** (Fig. 23) for Pd^{2+} sensing (Jiang et al. 2011). In 10 mM acetonitrile–water solution (CH_3CN:H_2O = 4:1, $NaBH_4$-PPh_3), there was a decrement in the fluorescence intensity upon treatment of compound **51** with Pd^{2+} (Fig. 23) in the presence of other tested metal ions. The detection of Pd^{2+} with **51** was linear within the concentration range of 0–1 μM. The detection limit of **51** for Pd^{2+} monitoring was calculated to be 6.1 nM. The practical utility of

Fig. 23 Structures of **49**–**51**

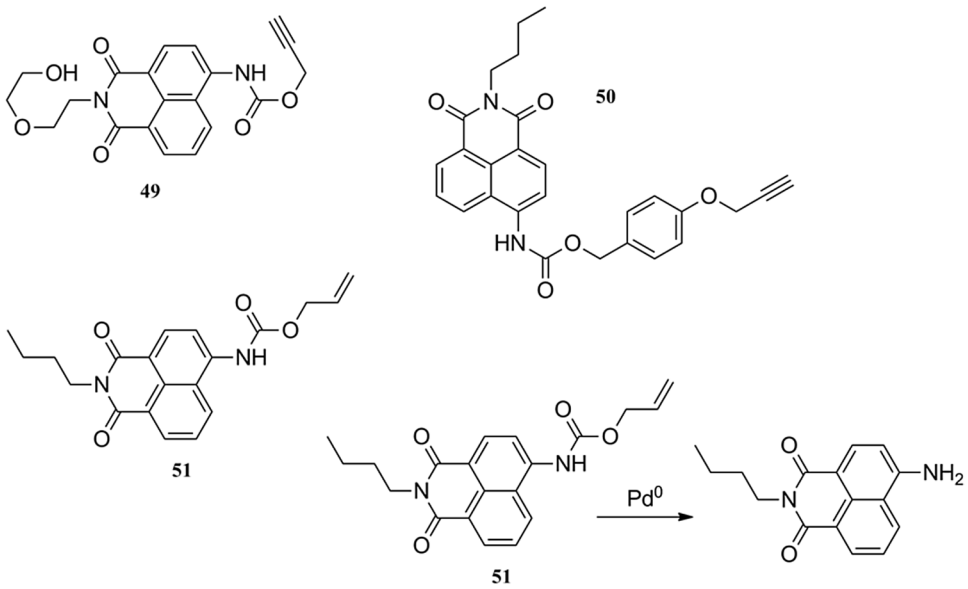

the synthesised compound was realised by its effective monitoring of Pd^{2+} concentrations in real-world pool and tap water samples.

Al^{3+}-selective chemosensor

Wang et al. synthesised the 1, 8-naphthalimide derivative **52** as a PET fluorescent chemosensor for Al^{3+} detection (Fig. 24) (Wang et al. 2017). When the fluorescence sensing property of the compound was tested in HEPES (PH = 7.4)/DMF (v/v, 1:1) solution that contained several cations including Al^{3+}, only Al^{3+} induced significant fluorescence enhancement on **52**. It was portrayed by the fluorescence plot that the compound exhibited good linearity within the concentration range of 3–11 μM. The detection limit and association constant of **52** interaction with Al^{3+} were calculated to be 3.4×10^{-8} M and 1×10^{4} M^{-1}, respectively. Experimental results of Job's plot and other titration analyses indicated the formation of a 1:1 stoichiometric complex between **52** and Al^{3+}. Desirably, a reversible complexation mode was achieved between the designed compound and Al^{3+} and the compound was successfully employed for Al^{3+} tracking in real water samples.

Recently, Li's research group reported the novel naphthalimide-appended chemosensor **53** whose fluorescence behaviour was taken advantage of to selectively and sensitively detect Al^{3+} amongst several other cations present under the same standard testing conditions (Li et al. 2017). In methanol (2.0×10^{-5} mol L^{-1}) and at 590 nm emission wavelength, 20-fold fluorescence amplification was observed by **53** when Al^{3+} was added. Contrastingly, this observation was not exhibited by other investigated competitive cations. High binding constant of 2.55×10^{5} mol^{-1} L of **53** (Fig. 24) towards Al^{3+} was obtained and low detection limit of 1.75×10^{-7} mol L^{-1} of **53** for Al^{3+} was estimated. What is more important, the reported compound enjoyed interesting application in the construction of logic circuit.

The effective 1, 8-naphthalimide-based chemosensor **54** that utilised both ICT and CHEF sensing mechanisms for Al^{3+} detection was reported by Kang and co-workers (Fig. 24) (Kang et al. 2016). The fluorescence titration experiment of the chemosensor for Al^{3+} monitoring in an array of other co-cations was conducted in CH_3OH solvent system. No significant fluorescence modulation was observed for ions investigated, except for 31.4-fold fluorescence enhancement noticed in the case of Al^{3+}. The competition experiment yielded the same trend of observation, demonstrating the remarkable ability of the chemosensor for singular sensing of Al^{3+} amongst other metal ions. The linear range of response was between 8 and 13 μM, with high association constant of 7.6×10^{4} M^{-1} and low detection limit of 6.9 μM calculated. Compound **54** was reversible in its detection mechanism and was consequently applied to sequester Al^{3+} from other cations in actual environmental system of some water samples.

Au^{3+} ion-selective chemosensors

Li et al. in 2016 designed two structurally similar 1, 8-naphthalimide-based derivatives, **57** and **58** (Fig. 25), bearing 4-*N*, *N*-dimethyl unit, as fluorescent chemosensors for Au^{3+} monitoring (Li et al. 2016). The reported compounds were well selective for Au^{3+} detection in H_2O–ethanol solution, displaying enhanced fluorescence responses towards Au^{3+} in the presence of 24 other metal ions tested under similar standard conditions. Compounds **57** and **58** exhibited 145-fold and 14-fold enhancements, respectively, in the magnitudes of their fluorescence intensities. The

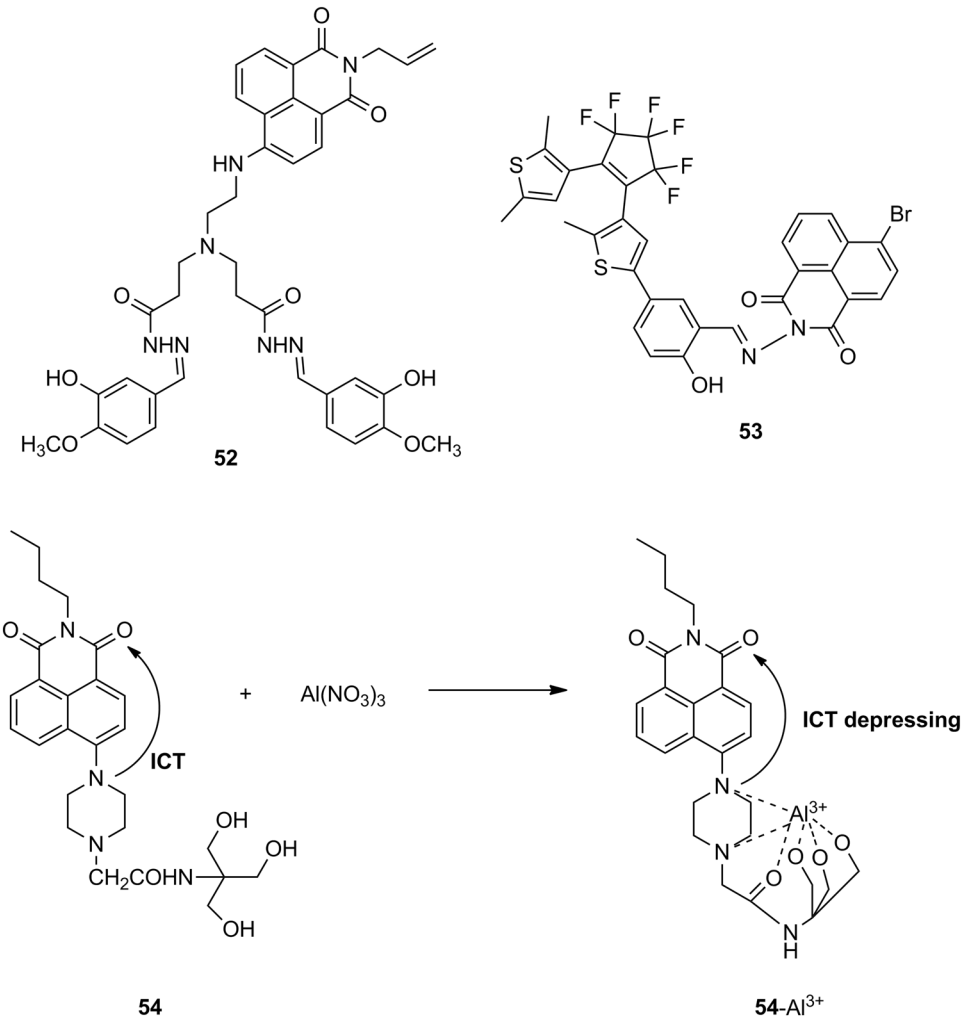

Fig. 24 Structures of **52** and **53** (up) and structure of **54** illustrating its sensing mechanism (down)

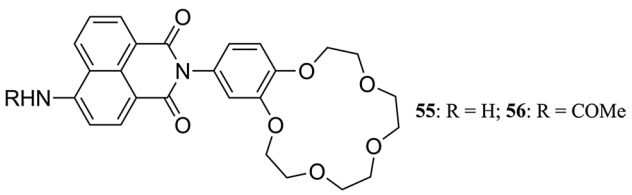

Fig. 25 Structures of **55** and **56**

detection limit of **57** for Al^{3+} monitoring was 0.050 μM while that of **58** was one-third of that of **57**. Results showed that chemosensor **57** exhibited better sensing properties than its counterpart, chemosensor **58**, but only **58** could be employed for Au^{3+} imaging in living cells.

Ba^{2+} ion-selective chemosensors

Panchenko et al. explored Ba^{2+}-sensing characteristics of the two naphthalimide derivatives **55** (that bears an *N*-phenyl-4-amino- unit) and **56** (which anchors an *N*-phenyl-4-acetamido- unit), both being appended with *N*-benzocrown ether fragment (Fig. 26) (Panchenko et al. 2010). In acetonitrile solution, gradual addition of Ba^{2+} solution to chemosensor **55** first led to initial fluorescence enlargement, then seconded by sudden reversal of the fluorescence intensity of **55** as the amount of Ba^{2+} was further increased. For **56**, there was significant amplification of its fluorescence intensity upon the addition of Ba^{2+} without any reversal observed as in the case of **55**.

Bi^{3+}-selective chemosensor

Kavitha and co-workers recently reported the novel compound **59** designed as a PET chemosensor for Bi^{3+} monitoring (Ramasamy and Thambusamy 2017). The best working pH of **59** for tracking Bi^{3+} was within the range 5–9. There was massive upward shift in the fluorescence intensity of chemosensor **59** upon interaction with Bi^{3+} in aqueous medium (5×10^{-5} M) in the concurrent presence of other metal ions. From the analysis of Job's plot,

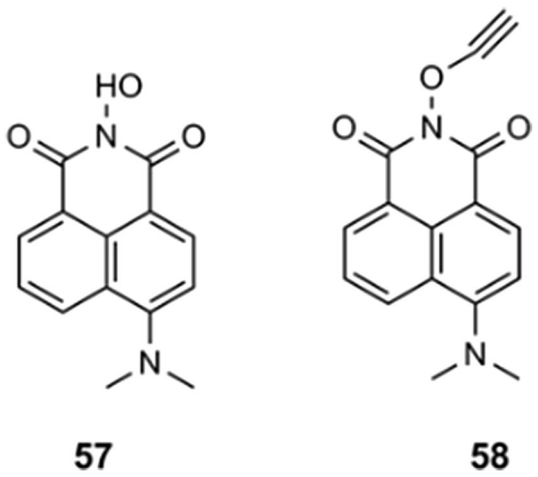

Fig. 26 Structures of **57** and **58**

the binding stoichiometry of **59** with Bi^{3+} (Fig. 27) was established to be 1:1. The association constant and detection limit were obtained as 311 M^{-1} and 0.58 μg mL^{-1}, respectively.

Multi-ion-selective chemosensors

Liu and teammates reported the novel naphthalimide-based ratiometric, fluorescent chemosensor **60** for the selective and sensitive detection of Fe^{3+} and Hg^{2+} (Fig. 28) (Liu and Qian 2017). The best working pH of compound **60** was confined to the narrow range of 2.92–4.5. When each of Fe^{3+} and Hg^{2+} cations was added to the chemosensor in acetonitrile/H_2O (v/v, 7:3) solution, the fluorescence intensity of **60** experienced sharp increase at the expense of those of other metal ions. Job's plot analysis yielded a 2:3 binding ratio of compound **60** with each of Fe^{3+} and Hg^{2+} ions. The calculated detection limits of **60** for Fe^{3+} and Hg^{2+} sensing are 2.72×10^{-8} and 9.08×10^{-8} M, respectively, while the calculated dissociation constants of the binding of **60** with

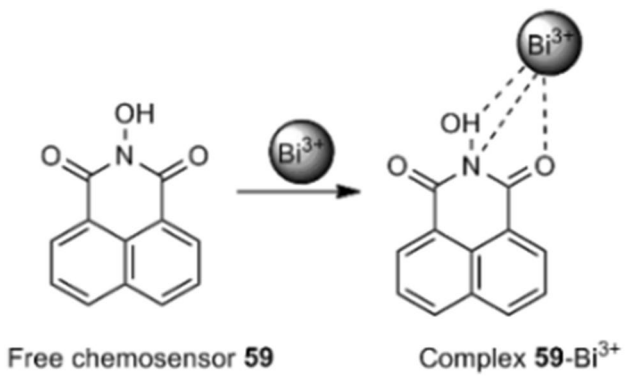

Fig. 27 Proposed binding mechanism of **59** with Bi^{3+}

Fe^{3+} and Hg^{2+} are 4.95×10^{-7} $M^{3/2}$ and 6.68×10^{-8} $M^{3/2}$, respectively. It was reported that compound **60** displayed excellent reversibility in its sensing of Fe^{3+} and Hg^{2+}.

Georgiev's research team reported the PET, FRET and ICT chemosensor **61** that bears 1, 8-naphthalimide fluorophore, which is sensitive and selective first for H^+ detection, and second for Cu^{2+} and Hg^{2+} monitoring in water/acetonitrile (v/v, 4:1) (Fig. 28) (Georgiev et al. 2015). There was upward rise of the fluorescence intensity of **61** upon addition of Cu^{2+} to solution of the compound in coexistence with other metal ions. The fluorescence response of the chemosensor with Cu^{2+} fell within the linear range of 2–10 μM while the limit of detection was obtained to be 0.5 μM. The binding stoichiometry as provided by Job's plot analysis was 1:1. The fluorescence emission of the compound was grossly reduced upon gradual addition of Hg^{2+} in the presence of other metal ions in water/acetonitrile (4:1, v/v), which was accrued to the 'switching on' of the fluorescence resonance energy transfer (FRET) process. The linear range of fluorescence response of **61** to Hg^{2+} was 2–20 μM while the detection limit was obtained to be 0.09 μM.

Janakipriya's group synthesised the fluorescence 'turn-on' PET-induced naphthalimide-based chemosensor **62** for the sensing of three trivalent metal ions, specifically, Fe^{3+}, Al^{3+} and Cr^{3+} (Fig. 28) (Janakipriya et al. 2016). Results of the Job's plot analysis revealed that Fe^{3+}, Al^{3+} and Cr^{3+} ions existed in a 1:1 binding ratio in complexes **62**-Fe^{3+}, **62**-Al^{3+} and **62**-Cr^{3+}, respectively. The detection limits of **62** were estimated to be 3.5×10^{-7}, 3.6×10^{-7} and 3.8×10^{-7} M, respectively, for Fe^{3+}, Al^{3+} and Cr^{3+} ions. The association constants were calculated as 3.8×10^4, 3.5×10^4 and 2.0×10^4 M^{-1}, respectively, for **62**-Fe^{3+}, **62**-Al^{3+} and **62**-Cr^{3+} complexes. In aqueous medium of H_2O:CH_3CN (9:1, v/v), addition of several other metal ions impacted no marked influence on the fluorescence emission intensity of **62**, except for Fe^{3+}, Al^{3+} and Cr^{3+} that induced significant fluorescence enhancement. The effectiveness of the compound was appraised in biological monitoring of the three metal ions, i.e. Fe^{3+}, Al^{3+} and Cr^{3+} in human keratinocyte (HaCaT) cells within the pH range of 6.0–9.2.

Zhang et al. came up with the stable 1, 8-naphthalimide-thiourea conjugate **63** used first for colourimetric detection of Fe^{3+} and Pb^{2+} and second for fluorescent recognition of Hg^{2+} (Fig. 28) (Zhang et al. 2014b). The colourimetric detections of Fe^{3+} and Pb^{2+} by **63** were carried out in MeCN/H_2O (99:1, v/v) while the fluorescent detection of Hg^{2+} was conducted in MeCN/H_2O (v/v, 85:15). In each of the two solvent systems utilised, the chemosensor selectively and sensitively tracked Fe^{3+}, Pb^{2+}, and Hg^{2+} in cohabitation with other rival cations, yielding 'turn on' fluorescence effects in both cases. The linear ranges of colourimetric and fluorescence responses for Fe^{3+}, Pb^{2+}, and Hg^{2+} were 0–150, 0–80, and 0–90 μM, respectively. The calculated detection

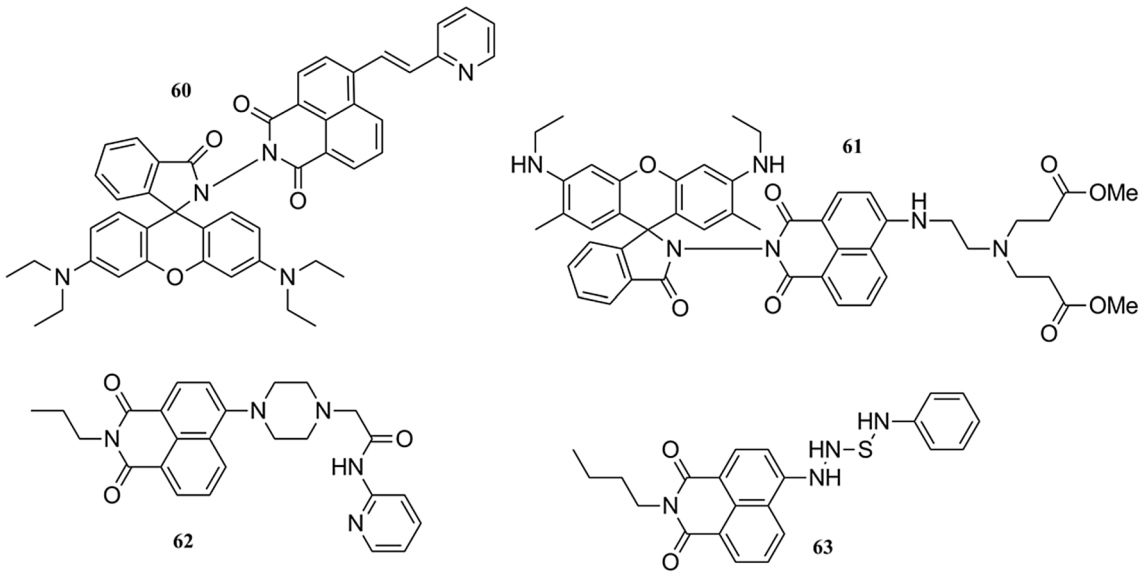

Fig. 28 Structures of **60–63**

limits of the designed compound for Fe^{3+}, Pb^{2+}, and Hg^{2+} were 6.86 μM, 5.09 μM, and 82.1 nM, respectively, while the obtained association constants of interaction of the reported compound with Fe^{3+}, Pb^{2+}, and Hg^{2+} were 1.854×10^3, 4.961×10^3, and 6.33×10^3 M^{-1}, respectively. The monitoring of these three ions, i.e. Fe^{3+}, Pb^{2+}, and Hg^{2+} was reversible as demonstrated by the freeing of the chemosensor upon the addition of EDTA solution to the metal complexes. Job's plot analysis indicated a 1:1 binding ratio of **63** for the three cations. Ultimately, the chemosensor was demonstrated for its practical effectiveness for Hg^{2+} tracking in pond and tap water samples and intracellular Hg^{2+} imaging in living cells.

Chemosensors that exhibit simultaneous fluorescence 'turn on' response for one metal ion and fluorescence 'turn off' response for another allow for the possibility of multication detection. Compound **64** developed by Huang et al.

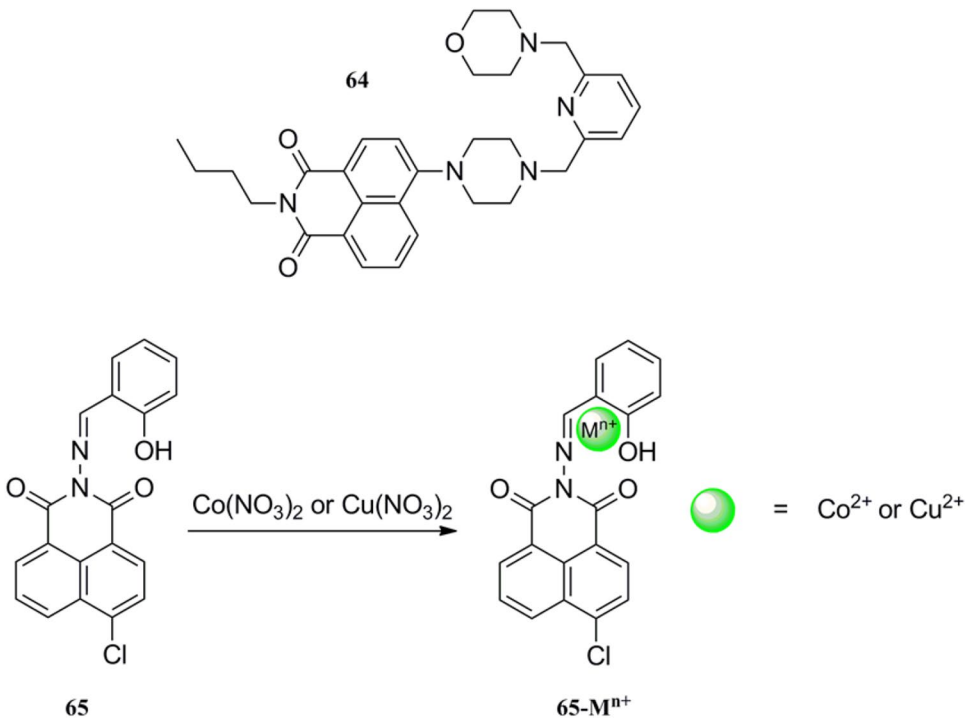

Fig. 29 Structure of **64** (up) and structure of **65** showing its binding mode with Co^{2+} or Cu^{2+} (down)

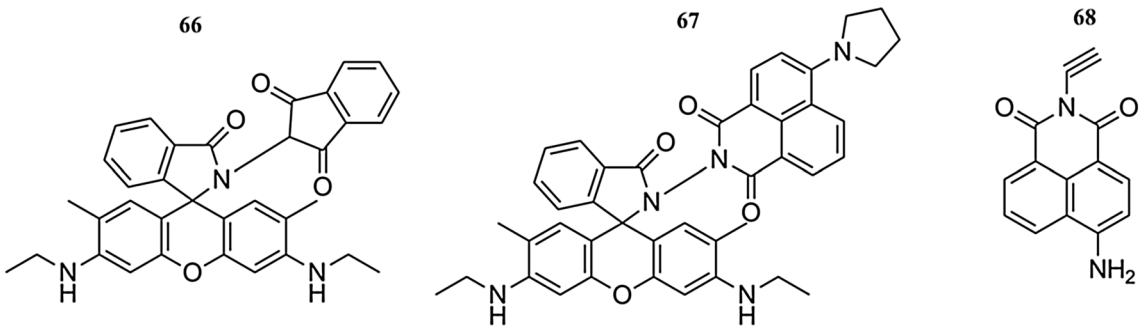

Fig. 30 Structures of **66–68**

(Fig. 29) is a typical example of such chemosensors (Huang et al. 2014b). **64** displayed fluorescence enhancement towards Hg^{2+} but fluorescence quenching towards Cu^{2+} in aqueous solution (10 mM HEPES, pH 7.5) in the presence of other cations. The strength of binding between the documented compound and investigated ions was justified by their high association constants of 6.06×10^6 and 3.51×10^6 M^{-1}, respectively. Job's plot revealed the formation of 1:1 complexes between **64** and each of the two metal ions. The binding mode was based on PET and CHEF mechanisms.

Sharma and co-workers synthesised the naphthalimide derivative **65**, commendable as chemosensor for Co^{2+} and Cu^{2+} detection (Fig. 29) (Sharma et al. 2012). In HEPES-buffered DMF/H_2O (8:2, v/v) solution, only Co^{2+} and Cu^{2+} induced massive lowering of the fluorescence intensity of the reported compound in the presence of other cations. Job's method of continuous variation corroborated a 1:1 binding ratio of **65** with Cu^{2+} and Co^{2+}. The calculated association constant of **65**-Co^{2+} and **65**-Cu^{2+} complexes were obtained to be $1.69 (\pm 0.1) \times 10^2$ and $2.9 (\pm 0.1) \times 10^2$ M^{-1}, respectively. It was shown that the reported compound **65** could be efficiently employed for detecting Cu^{2+} and Co^{2+} in solutions where they are present in a 1:2 ratio. The designated compound **65** proved applicable for the detection of Cu^{2+} and Co^{2+} in Osteosarcoma cells.

The two naphthalimide derivatives **66** and **67** were developed by Mahato et al. (Fig. 30) (Mahato et al. 2012). The compounds were selective and sensitive for monitoring Hg^{2+} or Cr^{3+} in the presence of several other competing metal ions. In CH_3CN-1.0 mM aq. HEPES buffer (pH = 7.2; 1:1, v/v), only Hg^{2+} and Cr^{3+} induced marked increase in the fluorescence intensities of **66** and **67**. This phenomenon was not observed in the case of other investigated ions. Reversible binding properties of **66** and **67** were successfully demonstrated for both Hg^{2+} and Cr^{3+}. A binding stoichiometry of 1:1 was given by Job's plot for the interaction of Hg^{2+} or Cr^{3+} with **66** or **67**. The respective emission binding constants of the reported compound **66** for the detections of Hg^{2+} and Cr^{3+} ions are $(3.07 \pm 0.3) \times 10^5$ and $(1.28 \pm 0.08) \times 10^5$ M^{-1}. Meanwhile, the emission binding constants determined for Hg^{2+} and Cr^{3+} by the reported compound **67** are $(1.12 \pm 0.01) \times 10^5$ and $(1.09 \pm 0.02) \times 10^5$ M^{-1}, respectively. Furthermore, the calculated detection limits of **66** for Hg^{2+} and Cr^{3+} were 0.35 and 0.14 ppb, respectively. Only chemosensor **67**, which worked optimally under physiological conditions, could be used for the imaging of Hg^{2+} and Cr^{3+} ions in living human epidermoid A431 cells.

Dong et al. brought to research limelight the 1, 8-naphthalimide-appended derivative that acted as an effective chemosensor for Hg^{2+} and Au^{3+} tracking in HEPES buffer (0.01 M; pH 7.4; 0.05% DMSO, v/v) (Fig. 30) (Dong et al. 2010). The fluorescence emission intensity of **68** plummeted upon the addition of Hg^{2+} to solution of compound **68**. Contrastingly, the addition of other coexisting ions impinged no great influence on the fluorescence intensity of compound **68**, which lend weight to the great selectivity of **68** for Hg^{2+}. The detection limit of **68** for Hg^{2+} sensing was determined to be 0.05 μM (10 ppb). The reported compound was successfully envisaged as an excellent chemosensor for Au^{3+} monitoring amongst several other metal ions tested.

Although there is no room for detailed discussion, additional published works to the use of 1, 8-naphthalimide for the constructions of fluorescent and colourimetric chemosensors are cited (Saini et al. 2014; Zhang et al. 2017; Un et al. 2014b; Aderinto et al. 2016; Wu et al. 2013; Hou et al. 2011; Chen et al. 2012; Liu et al. 2012b; Duan et al. 2008; Zhang et al. 2010; Chinapang et al. 2015; Zhang et al. 2012; Chen et al. 2013a; Hu et al. 2014; Zhang et al. 2011a; Yu et al. 2012; Yu and Zhang 2014; Choi et al. 2013).

Conclusions

The successfulness of the robust fluorophore, 1, 8-naphthalimide, which exists often as 4-amino-1, 8-naphthalimide for the constructions of diverse fluorescent chemosensors of interesting applications in environmental- and biological systems, is intriguing. In this review, various representative

Table 1 A few key parameters of the fluorescent and colourimetric chemosensors covered in this review

Chemosensor number	Analyte (s) detected	Detection limit (mol L^{-1})	Environmental and/or biological application	References
1	Cu^{2+}	2.40×10^{-6}	N.R.[a]	Fu et al. (2017b)
2	Cu^{2+}	1.30×10^{-8}	Aqueous solution and HeLa cells	Gao et al. (2016)
3	Cu^{2+}	3.26×10^{-8}	Living HeLa cells	Chen et al. (2016)
4	Cu^{2+}	2.30×10^{-7}	N.R.	Xu et al. (2017)
5	Cu^{2+}	6.40×10^{-8}	MCF-7 cells	He et al. (2015)
6	Cu^{2+}	5.20×10^{-8}	Water samples	Hu et al. (2015)
7	Cu^{2+}	2.50×10^{-8}	Water samples	Yu and Zhang (2014)
8	Cu^{2+}	1.50×10^{-8}	N.R.	Chen et al. (2013b)
9	Cu^{2+}	4.80×10^{-8}	N.R.	Lan et al. (2012)
10	Cu^{2+}	N.R.	N.R.	Lan et al. (2012)
11	Cu^{2+}	N.R.	N.R.	Georgiev and Bojinov (2012)
12	Cu^{2+}	1.80×10^{-7}	Living cells	Yu et al. (2011)
13	Cu^{2+}	N.R.	N.R.	Xu et al. (2010d)
14	Cu^{2+}	1.00×10^{-8}	N.R.	Xu et al. (2010b)
15	Cu^{2+}	1.00×10^{-8}	N.R.	Xu et al. (2010b)
16	Hg^{2+}	2.40×10^{-7}	N.R.	La et al. (2016)
17	Hg^{2+}	2.10×10^{-6}	N.R.	Li et al. (2012a)
18	Hg^{2+}	3.10×10^{-6}	N.R.	Li et al. (2012b)
19	Hg^{2+}	N.R.	Living mammalian cells	Vonlanthen et al. (2014)
20	Hg^{2+}	6.28×10^{-8}	Living HeLa cells	Un et al. (2014a)
21	Hg^{2+}	2.70×10^{-6}	N.R.	Moon et al. (2013)
22	Hg^{2+}	N.R.	N.R.	Moon et al. (2013)
23	Hg^{2+}	N.R.	N.R.	Moon et al. (2013)
24	Hg^{2+}	1.27×10^{-6}	N.R.	Zhang et al. (2013a)
25	Hg^{2+}	4.93×10^{-8}	Hair samples	Li et al. (2012a)
26	Hg^{2+}	6.30×10^{-8}	N.R.	Yang et al. (2012)
27	Hg^{2+}	N.R.	Living HeLa cells	Li et al. (2012b)
28	Hg^{2+}	3.00×10^{-8}	N.R.	Liu et al. (2012a)
29	Hg^{2+}	2.00×10^{-6}	Prostate cancer cell lines	Kumar et al. (2011)
30	Cr^{3+}	6.00×10^{-7}	Live HeLa cells	Yu et al. (2016)
31	Cr^{3+}	N.R.	N.R.	Xue et al. (2015)
32	Cr^{3+}	2.00×10^{-7}	N.R.	Wu et al. (2014)
33	Fe^{3+}	3.88×10^{-7}	N.R.	Li et al. (2014)
34	Fe^{3+}	3.00×10^{-8}	W138 human lung fibroblast cells	Chereddy et al. (2014)
35	Fe^{3+}	4.69×10^{-7}	N.R.	Yang et al. (2013)
36	Fe^{3+}	4.50×10^{-6}	Pharmaceutical preparation samples	Xu et al. (2013)
37	Fe^{3+}	2.00×10^{-7}	N.R.	Staneva et al. (2012)
38	Zn^{2+}	7.20×10^{-9}	Living HeLa cells	Wei et al. (2015)
39	Zn^{2+}	N.R.	Living cells	Liu et al. (2014)
40	Zn^{2+}	1.03×10^{6}	A549, BEAS-2B CHO, HeLa, and HepG2cells	Zhao et al. (2013)
41	Zn^{2+}	1.10×10^{-9}	HeLa cells	Hanaoka et al. (2010)
42	Zn^{2+}	N.R.	N.R.	Xu et al. (2010a)
43	Zn^{2+}	N.R.	N.R.	Tamanini et al. (2010)
44	Zn^{2+}	N.R.	N.R.	Tamanini et al. (2010)
45	Ag^{+}	N.R.	N.R.	Fu et al. (2016)
46	Ag^{+}	3.00×10^{-6}	N.R.	Zhou et al. (2012)
47	Ag^{+}	N.R.	N.R.	Xu et al. (2010e)

Table 1 (continued)

Chemosensor number	Analyte (s) detected	Detection limit (mol L^{-1})	Environmental and/or biological application	References
48	Ag^{+}	1.00×10^{-8}	N.R.	Xu et al. (2010e)
49	Pd^{2+}	2.50×10^{-8}	Hep G2 and HL60 living cells	Liu et al. (2014)
		2.70×10^{-6}		
50	Pd^{2+}	N.R.	N.R.	Wang et al. (2012)
51	Pd^{2+}	6.10×10^{-9}	Water samples	Jiang et al. (2011)
52	Al^{3+}	3.40×10^{-8}	Water samples	Wang et al. (2017)
53	Al^{3+}	1.75×10^{-7}	Molecular logic circuit	Li et al. (2017)
54	Al^{3+}	6.90×10^{-6}	Water samples	Kang et al. (2016)
55	Ba^{2+}	N.R.	N.R.	Panchenko et al. (2010)
56	Ba^{2+}	N.R.	N.R.	Panchenko et al. (2010)
57	Au^{3+}	5.00×10^{-8}	N.R.	Li et al. (2012a)
58	Au^{3+}	N.R.	Living cells	Li et al. (2016b)
59	Bi^{3+}	5.80×10^{-7}	N.R.	Ramasamy and Thambusamy (2017)
60	Fe^{3+}	2.72×10^{-8}	N.R.	Liu and Qian (2017)
	Hg^{2+}	9.08×10^{-8}	N.R.	
61	Cu^{2+}	5.00×10^{-7}	Logic gates and logic circuit	Georgiev et al. (2015)
	Hg^{2+}	9.00×10^{-8}		
62	Fe^{3+}	3.50×10^{-7}	Human keratinocyte (HaCaT)	Janakipriya et al. (2016)
	Al^{3+}	3.60×10^{-7}		
	Cr^{3+}	3.80×10^{-7}		
63	Fe^{3+}	6.86×10^{-6}	Water samples and living cells	Zhang et al. (2014b)
	Pb^{2+}	5.09×10^{-6}		
	Hg^{2+}	8.21×10^{-8}		
64	Hg^{2+}	6.11×10^{-8}	N.R.	Huang et al. (2014b)
	Cu^{2+}	N.R.	N.R.	
65	Co^{2+}	N.R.	Osteosarcoma cells and logic gates	Sharma et al. (2012)
	Cu^{2+}	N.R.		
66	Hg^{2+}	3.50×10^{-10}	N.R.	Mahato et al. (2011)
	Cr^{3+}	1.40×10^{-10}		
67	Hg^{2+}	N.R.	Living human epidermoid A431 cells	Mahato et al. (2011)
	Cr^{3+}	N.R.		
68	Hg^{2+}	5.00×10^{-8}	N.R.	Dong et al. (2010)
	Au^{3+}	N.R.		

[a]Where "N.R." means the parameter in question was "Not Reported"

1, 8-naphthalimide-based fluorescent chemosensors for selected cations (i.e. Cu^{2+}, Hg^{2+}, Cr^{3+}, Fe^{3+}, Zn^{2+}, Ag^{+}, Pd^{2+}, Al^{3+}, Ba^{2+}, Au^{3+}, and Bi^{2+}), and/or a combination of these metal ions, have been summarised. All reported chemosensors contained three essential parts: fluorophore, spacer, and receptor. Different mechanisms such as Photoinduced Electron Transfer (PET), Internal Charge Transfer (ICT), and Fluorescence Resonance Energy Transfer (FRET) were employed in the constructions of these naphthalimide derivatives, although details about these mechanisms have not been elucidated. For a summary of a few key parameters about chemosensors **1**–**68**, readers are referred to Table 1.

While a significant great success has been achieved in the developments of fluorescent and colourimetric 1, 8-naphthalimide-based chemosensors of interesting sensing parameters and great environmental- and biological application significances, much work still remains to be done. If researchers in this field continue to exert more efforts, it is foreseeable that chemosensors of improved sensing properties and practical application values that would meet future

demands of metal ion tracking would be generated, thereby revolutionising the field of sensing science.

Acknowledgements The work reported in this review would not have been a possibility without the scholarship supports benefitted from the China Scholarship Council (CSC Nos. 2014BSZ528 and 2017BSZ012726) which are not taken lightly.

References

Aderinto SO, Xu Y, Peng H, Wang F, Wu H, Fan X (2016) A highly selective fluorescent sensor for monitoring Cu^{2+} ion: synthesis, characterization and photophysical properties. J Fluoresc 27:79–87. https://doi.org/10.1007/s10895-016-1936-7

Anikin VF, Fedko NF (2006) Synthesis of ion-active naphthalimide derivatives. Russ J Org Chem 42:73–76. https://doi.org/10.1134/S107042800601012X

Bicker KL, Wiskur SL, Lavigne JJ (2011) Chemosensors: principles, strategies, and applications, 1st edn. Wiley, New York, pp 275–295

Bojinov V, Grabchev I (2003) Synthesis of new polymerizable 1,8-naphthalimide dyes containing a 2-hydroxyphenylbenzotriazole fragment. Dyes Pigm 59:277–283. https://doi.org/10.1016/S0143-7208(03)00113-X

Bojinov VB, Panova IP (2009) Novel 4-(2, 2, 6, 6-tetramethylpiperidin-4-ylamino)-1, 8- naphthalimide based yellow-green emitting fluorescence sensors for transition metal ions and protons. Dyes Pigm 80:61–66. https://doi.org/10.1016/j.dyepig.2008.05.007

Bojinov VB, Panova IP, Chovelon J-M (2008) Novel blue emitting tetra-and pentamethylpiperidin-4-yloxy-1, 8-naphthalimides as photoinduced electron transfer based sensors for transition metal ions and protons. Sens Actuators B: Chem 135:172–180. https://doi.org/10.1016/j.snb.2008.08.016

Bojinov VB, Georgiev NI, Bosch P (2009) Design and synthesis of highly photostable yellow-green emitting 1, 8-naphthalimides as fluorescent sensors for metal cations and protons. J Fluoresc 19:127–139. https://doi.org/10.1007/s10895-008-0394-2

Bricks JL, Kovalchuk A, Trieflinger C, Nofz M, Büschel M, Tolmachev AI, Daub J, Rurack K (2005) On the development of sensor molecules that display Fe^{III}-amplified fluorescence. J Am Chem Soc 127:13522–13529. https://doi.org/10.1021/ja050652t

Bryan AJ, de Silva AP, de Silva SA, Rupasinghe RADD, Sandanayake KRAS (1989) Photo-induced electron transfer as a general design logic for fluorescent molecular sensors for cations. Biosensors 4:169–179. https://doi.org/10.1016/0265-928X(89)80018-5

Burdette SC, Walkup GK, Spingler B, Tsien RY, Lippard SJJ (2001) Fluorescent sensors for Zn^{2+} based on a fluorescein platform: synthesis, properties and intracellular distribution. J Am Chem Soc 123:7831–7841

Carter KP, Young AM, Palmer AE (2014) Fluorescent sensors for measuring metal ions in living systems. Chem Rev 114(8):4564–4601. https://doi.org/10.1021/cr400546e

Chen Z, Wang L, Zou G, Teng M, Yu J (2012) Highly selective fluorescence turn-on chemosensor based on naphthalimide derivatives for detection of trivalent chromium ions. Chin J Chem 30:2844–2848. https://doi.org/10.1002/cjoc.201201070

Chen S, Hou P, Foley JW, Song X (2013a) A colorimetric and ratiometric fluorescent probe for Cu^{2+} with a large red shift and its imaging in living cells. RSC Advances 3:5591–5596. https://doi.org/10.1039/C3RA23057K

Chen Z, Wang L, Zou G, Tang J, Cai X, Teng M, Chen L (2013b) Highly selective fluorescence turn-on chemosensor based on naphthalimide derivatives for detection of copper(II) ions. Spectrochim Acta Mol Biomol Spectrosc 105:57–61. https://doi.org/10.1016/j.saa.2012.12.005

Chen J, Su W, Wang E, Liu Y (2016) 1,8-Naphthalimide-based turn-on fluorescent chemosensor for Cu^{2+} and its application in bioimaging. J Lumin 180:301–305. https://doi.org/10.1016/j.jlumin.2016.08.040

Chereddy NR, Raju MVN, Nagaraju P, Krishnaswamy VR, Korrapati PS, Bangal PR, Rao VJ (2014) A naphthalimide based PET probe with Fe^{3+} selective detection ability: theoretical and experimental study. Analyst 139:6352–6356. https://doi.org/10.1039/C4AN01528B

Chinapang P, Ruangpornvisuti V, Sukwattanasinitt M, Rashatasakhon P (2015) Ferro derivative of 1, 8-naphthalimide as a new turn-on fluorescent sensor for Au(III) ion. Dyes Pigm 112:236–238. https://doi.org/10.1016/j.dyepig.2014.07.013

Choi JY, Kim G-H, Guo Z, Lee HY, Swamy KMK, Pai J, Shin S, Shin I, Yoon J (2013) Highly selective ratiometric fluorescent probe for Au^{3+} and its application to bioimaging. Biosens Bioelectron 49:438–441. https://doi.org/10.1016/j.bios.2013.05.033

Chovelon J-M, Grabchev I (2007) A novel fluorescent sensor for metal cations and protons based of bis-1,8-naphthalimide. Spectrochimica Acta A 67:87–91. https://doi.org/10.1016/j.saa.2006.06.037

Cosnard F, Wintgens V (1998) A new fluoroionophore derived from 4-amino-N-methyl-1, 8-naphthalimide. Tetrahedron Lett 39:2751–2754. https://doi.org/10.1016/S00404039(98)00302-5

de Silva AP, Gunaratne HON, Lynch PLM (1995a) Luminescence and charge transfer. Part 4. 'On–off' fluorescent PET (photoinduced electron transfer) sensors with pyridine receptors: 1, 3-diaryl-5-pyridyl-4,5-dihydropyrazoles. J Chem Soc Perkin Trans 2:685–690. https://doi.org/10.1039/P29950000685

de Silva AP, Gunaratne HQN, Habib-Jiwan J-L, McCoy CP, Rice TE, Soumillion J-P (1995b) New fluorescent model compounds for the study of photoinduced electron transfer: the influence of a molecular electric field in the excited state. Angew Chem Int Edit Engl 34:1728–1731. https://doi.org/10.1002/anie.199517281

de Silva AP, Gunaratne HQN, Gunnlaugsson T, Lynch PLM (1996) Molecular photoionic switches with an internal reference channel for fluorescent pH sensing applications. New J Chem 20:871–880

de Silva AP, Gunaratne HQN, Gunnlaugsson T, Huxley AJM, McCoy CP, Rademacher JT, Rice TE (1997a) Novel 4-(2,2,6,6-tetramethylpiperidin-4-ylamino)-1,8-naphthalimide based yellow-green emitting fluorescence sensors for transition metal ions and protons. Chem Rev 97:1515–1566. https://doi.org/10.1016/j.dyepig.2008.05.007

de Silva AP, Gunaratne HQN, McCoy CP (1997b) Molecular photoionic AND logic gates with bright fluorescence and "off – on" digital action. J Am Chem Soc 119:7891–7892. https://doi.org/10.1021/ja9712229

de Souza MM, Correa R, Filho VC, Grabchev I, Bojinov V (2002) 4-Nitro-1,8-naphthalimides exhibit antinociceptive properties. Pharmazie 57:430–431

Deng M, Gong D, Han SC, Zhu X, Iqbal A, Liu W, Qin W, Guo H (2017) BODIPY based phenylthiourea derivatives as highly selective $MeHg^{+}$ and Hg^{2+} ions fluorescent chemodosimeter and its application to bioimaging. Sens Actuators B: Chem 243:195–202. https://doi.org/10.1016/j.snb.2016.11.13

Dey S, Sarkar S, Maity D, Roy P (2017) Rhodamine based chemosensor for trivalent cations: synthesis, spectral properties, secondary complex as sensor for arsenate and molecular logic gates. Sens Actuators B: Chem 246:518–534. https://doi.org/10.1016/j.snb.2017.02.094

Dong M, Wang Y-W, Peng Y (2010) Highly selective ratiometric fluorescent sensing for Hg^{2+} and Au^{3+}, respectively, in aqueous

media. Org Lett 12:5310–5313. https://doi.org/10.1021/ol1024585

Du J, Hu M, Fan J, Peng X (2012) Fluorescent chemodosimeters using "mild" chemical events for the detection of small anions and cations in biological and environmental media. Chem Soc Rev 41:4511–4535. https://doi.org/10.1039/C2CS00004K

Duan L, Xu Y, Qian X (2008) Highly sensitive and selective Pd^{2+} sensor of naphthalimide derivative based on complexation with alkynes and thio-heterocycle. Chem Commun 0:6339–6341. https://doi.org/10.1039/B815298E

Duke RM, Veale EB, Pfeffer FM, Kruger PE, Gunnlaugsson T (2010) Colorimetric and fluorescent anion sensors: an overview of recent developments in the use of 1,8- naphthalimide-based chemosensors. Chem Soc Rev 39:3936–3953. https://doi.org/10.1039/B910560N

Erdemir S, Kocyigit O (2017) A novel dye based on phenolphthalein-fluorescein as a fluorescent probe for the dual-channel detection of Hg^{2+} and Zn^{2+}. Dyes Pigm 145:72–79. https://doi.org/10.1016/j.dyepig.2017.05.053

Fan J, Peng X, Wu Y, Lu E, Hou J, Zhang H, Zhang R, Fu X (2005) A new PET fluorescent sensor for Zn^{2+}. J Lumin 114:125–130. https://doi.org/10.1016/j.jlumin.2004.12.008

Fu Y, Li P, Kang J-X, Liu X-Y, Li G-Y, Ye F (2016) A novel 1, 8-naphthalimide derivative as an efficient silver (I) fluorescent sensor. J Lumin 178:156–162. https://doi.org/10.1016/j.jlumin.2016.05.023

Fu ZH, Han X, Shao Y, Fang J, Zhang Z, Wang Y-W, Peng Y (2017a) Fluorescein-based chromogenic and ratiometric fluorescence probe for highly selective detection of cysteine and its application in bioimaging. Anal Chem 89:1937–1944. https://doi.org/10.1021/acs.analchem.6b04431

Fu Y, Fan C, Liu G, Pu S (2017b) A colorimetric and fluorescent sensor for Cu^{2+} and F^- based on a diarylethene with a 1, 8-naphthalimide Schiff base unit. Sens Actuators B: Chem 239:295–303. https://doi.org/10.1016/j.snb.2016.08.020

Gao Y-G, Tang Q, Shi Y-D, Zhang Y, Lu Z-L (2016) 1, 8-Naphthalimide modified [12]aneN_3 compounds as selective and sensitive probes for Cu^{2+} ions and ATP in aqueous solution and living cells. Talanta 152:438–446. https://doi.org/10.1016/j.talanta.2016.02.040

Georgiev NI, Bojinov VB (2012) Design, synthesis and sensor activity of a highly photostable blue emitting 1, 8-naphthalimide. J Lumin 132:2235–2241. https://doi.org/10.1016/j.jlumin.2012.04.023

Georgiev NI, Bojinov VB, Nikolov PS (2011) The design, synthesis and photophysical properties of two novel 1, 8-naphthalimide fluorescent pH sensors based on PET and ICT. Dyes Pigm 88:350–357. https://doi.org/10.1016/j.dyepig.2010.08.004

Georgiev NI, Dimitrova MD, Asiri AM, Alamry KA, Bojinov VB (2015) Synthesis, sensor activity and logic behaviour of a novel bichromophoric system based on rhodamine 6G and 1,8-naphthalimide. Dyes Pigm 115:172–180. https://doi.org/10.1016/j.dyepig.2015.01.001

Goncalves AC, Capelo JL, Lodeiro C, Santos AAD (2017) A selenopyrene selective probe for Hg^{2+} detection in either aqueous or aprotic systems. Sens Actuators B: Chem 239:311–318. https://doi.org/10.1016/j.snb.2016.08.014

Gonçalves AC, Martinez JLC, Lodeiro C, Santos AAD (2017) A selective emissive chromogenic and fluorogenic seleno-coumarin probe for Cu^{2+} detection in aprotic media. Photochem Photobiol Sci 16:1174–1181. https://doi.org/10.1039/C7PP00036G

Grabchev I, Chovelon JM (2003) Synthesis and functional properties of green fluorescent poly (methylmethacrylate) for use in liquid crystal systems. Polym Adv Technol 14:601–608. https://doi.org/10.1002/pat.376

Grabchev I, Chovelon J-M (2008) New blue fluorescent sensors for metal cations and protons based on 1, 8-naphthalimide. Dyes Pigm 77:1–6. https://doi.org/10.1016/j.dyepig.2007.02.012

Grabchev I, Meallier P, Konstantinova T, Popova M (1995) Synthesis of some unsaturated 1, 8-naphthalimide dyes. Dyes Pigm 28:41–46. https://doi.org/10.1016/0143-7208(94)00078-G

Grabchev I, Chovelon J-M, Qian X (2003) A copolymer of 4-N, N-dimethylaminoethylene-N-allyl-1,8-naphthalimide with methylmethacrylate as a selective fluorescent chemosensor in homogeneous systems for metal cations. J Photochem Photobiol A Chem 158:37–43. https://doi.org/10.1016/S1010-6030(03)00100-X

Grabchev I, Soumillion JP, Muls B, vanova G (2004) Poly (amidoamine) dendrimer peripherally modified with 4-N, N-dimethylaminoethyleneamino-1, 8-naphthalimide as a sensor of metal cations and protons. Photochem Photobiol Sci 3:1032–1037. https://doi.org/10.1039/B412384K

Gruzinskii VV, Kukhto AV, Shakkah GKh (1998) Spectra of lasing efficiency in lasers with solutions of complex organic compounds. J Appl Spectrosc 65:463–465

Gunnlaugsson T, Lee TC, Parkesh R (2003) A highly selective and sensitive fluorescent PET (photoinducedelectron transfer) chemosensor for Zn(II). Org Biomol Chem 1:3265–3267. https://doi.org/10.1039/B309569J

Gunnlaugsson T, Glynn M, Tocci GM, Kruger PE, Pfeffer FM (2006) Anion recognition and sensing in organic and aqueous media using luminescent and colorimetric sensors. Coord Chem Rev 250:3094–3117. https://doi.org/10.1016/j.ccr.2006.08.017

Gupta RC, Razi SS, Ali R, Diwivedi SK, Srivastava P, Singh P, Koch B, Mishra H, Misra A (2017) An efficient Hg^{2+} ensemble based on a triazole bridged anthracene and quinoline system for selective detection of cyanide through fluorescence turn-off–on response in solution and live cell. Sens Actuators B: Chem 251:729–738. https://doi.org/10.1016/j.snb.2017.04.096

Hanaoka K, Muramatsu Y, Urano Y, Terai T, Nagano T (2010) Design and synthesis of a highly sensitive off–on fluorescent chemosensor for zinc ions utilizing internal charge transfer. Chemistry 16:568–572. https://doi.org/10.1002/chem.200901591

He H, Mortellaro MA, Leiner MJP, Fraatz RJ, Tusa JK (2003) A fluorescent sensor with high selectivity and sensitivity for potassium in water. J Am Chem Soc 125:1468–1469. https://doi.org/10.1021/ja0284761

He G, Meng Q, Zhao X, He C, Zhou P, Duan C (2015) A new copper (II) selective fluorescence probe based on naphthalimide: synthesis, mechanism and application in living cells. Inorg Chem Commun 65:28–31. https://doi.org/10.1016/j.inoche.2015.10.022

Hou C, Urbanec AM, Cao H (2011) A rapid Hg^{2+} sensor based on aza-15-crown-5 ether functionalized 1, 8-naphthalimide. Tetrahedron Lett 52:4903–4905. https://doi.org/10.1016/j.tetlet.2011.07.056

Hou L, Feng J, Wang Y, Dong C, Shuang S, Wang Y (2017) Single fluorescein-based probe for selective colorimetric and fluorometric dual sensing of Al^{3+} and Cu^{2+}. Sens Actuators B: Chem 247:451–460. https://doi.org/10.1016/j.snb.2017.03.027

Hu F, Zheng B, Wang D, Liu M, Du J, Xiao D (2014) A novel dual-switch fluorescent probe for Cr(III) ion based on PET–FRET processes. Analyst 139:3607–3613. https://doi.org/10.1039/C4AN00303A

Hu X-X, Zheng X-L, Fan X-X, Su Y-T, Zhan X-Q, Zheng H (2015) Semicarbazide-based naphthalimide as a highly selective and sensitive colorimetric and "turn-on" fluorescent chemodosimeter for Cu^{2+}. Sens Actuators B: Chem 227:191–197. https://doi.org/10.1016/j.snb.2015.12.037

Huang C, Jia T, Tang M, Yin Q, Zhu W, Zhang C, Yang Y, Jia N, Xu Y, Qian X (2014a) Selective and ratiometric fluorescent trapping and quantification of protein vicinal dithiols and in situ dynamic

tracing in living cells. J Am Chem Soc 136:14237–14244. https://doi.org/10.1021/ja5079656

Huang C-B, Li H-R, Luo Y, Xu L (2014b) A naphthalimide-based bifunctional fluorescent probe for the differential detection of Hg^{2+} and Cu^{2+} in aqueous solution. Dalton Trans 43:8102–8108. https://doi.org/10.1039/C4DT00014E

Huang K, Jiao X, Liu C, Wang Q, Qiu X, Zheng D, He S, Zhao L, Zeng X (2017) Highly selective and sensitive fluorescent probe for mercury ions based on a novel rhodol-coumarin hybrid dye. Dyes Pigm 142:437–446. https://doi.org/10.1016/j.dyepig.2017.04.005

Janakipriya S, Chereddy NR, Korrapati P, Thennarasu S, Mandal AB (2016) Selective interactions of trivalent cations Fe^{3+}, Al^{3+} and Cr^{3+} turn on fluorescence in a naphthalimide based single molecular probe. Spectrochima Acta Mol Biomol Spectrosc. https://doi.org/10.1016/j.saa.2015.08.044

Jiang J, Jiang H, Liu W, Tang X, Zhou X, Liu W, Liu R (2011) A colorimetric and ratiometric fluorescent probe for palladium. Org Lett 13:4922–4925. https://doi.org/10.1021/ol202003j

Jiang C, Wang M, Wang Y, Tang X, Zhang Y, Zhang H, Ma L, Wang J (2017) Synthesis and evaluation of two novel rhodamine-based fluorescence probes for specific recognition of Fe^{e+} ion. Tetrahedron Lett 58:2560–2565. https://doi.org/10.1016/j.tetlet.2017.05.052

Kang L, Xing Z-Y, Ma X-Y, Liu Y-T, Zhang Y (2016) A highly selective colorimetric and fluorescent turn-on chemosensor for Al^{3+} based on naphthalimide derivative. Spectrochima Acta Mol Biomol Spectrosc 167:59–65. https://doi.org/10.1016/j.saa.2016.05.030

Kim HN, Lee MH, Kim HJ, Kim JS, Yoon J (2008) A new trend in rhodamine-based chemosensors: application of spirolactam ring-opening to sensing ions. Chem Soc Rev 37:1465–1472. https://doi.org/10.1039/b802497a

Kim HN, Ren WX, Kim JS, Yoon J (2012) Fluorescent and colorimetric sensors for detection of lead, cadmium, and mercury ions. Chem Soc Rev 41:3210–3244. https://doi.org/10.1039/C1CS15245A

Kim KT, Yoon SA, Ahn J, Choi Y, Lee MH, Jung JH, Park J (2017) Synthesis of fluorescent naphthalimide-functionalized Fe_3O_4 nanoparticles and their application for the selective detection of Zn^{2+} present in contaminated soil. Sens Actuators B: Chem 243:1034–1041. https://doi.org/10.1016/j.snb.2016.11.131

Kumar M, Kumar N, Bhalla V, Singh H, Sharma PR, Kaur T (2011) Naphthalimide appended rhodamine derivative: through bond energy transfer for sensing of Hg^{2+} ions. Org Lett 13:1422–1425. https://doi.org/10.1021/ol2001073

La YK, Hong JA, Jeong YJ, Lee J (2016) A 1,8-naphthalimide-based chemosensor for dual-mode sensing: colorimetric and fluorometric detection of multiple analytes. RSC Advances 6:84098–84105. https://doi.org/10.1039/c6ra20100h

Lakowicz JR (2006) Principles of fluorescent spectroscopy, 3rd edn. Springer, New york

Lan H, Liu B, Lv G, Li Z, Yu X, Liu K, Cao X, Yang H, Yang S, Yi T (2012) Dual-channel fluorescence "turn on" probe for Cu^{2+}. Sens Actuators B: Chem 173:811–816. https://doi.org/10.1016/j.snb.2012.07.102

Law KY (1993) Organic photoconductive materials: recent trends and developments. Chem Rev 93:449–486. https://doi.org/10.1021/cr00017a020

Lee MH, Yoon B, Kim JS, Sessler JL (2013) Naphthalimide trifluoroacetyl acetonate: a hydrazine-selective chemodosimetric sensor. Chem Sci 4:4121–4126. https://doi.org/10.1039/C3SC51813B

Lee MH, Jeon HM, Han JH, Park N, Kang C, Sesser JL, Kim JS (2014) Toward a chemical marker for inflammatory disease: a fluorescent probe for membrane-localized thioredoxin. J Am Chem Soc 136(23):8430–8437. https://doi.org/10.1021/ja503356q

Lee MH, Kim JS, Sessler JL (2015) Small molecule-based ratiometric fluorescence probes for cations, anions, and biomolecules. Chem Soc Rev 44:4185–4191. https://doi.org/10.1039/C4CS00280F

Li CY, Zhang XB, Qiao L, Zhao Y, He CM, Huan SY, Lu LM, Jian LX, Shen GL, Yu RQ (2009) Naphthalimide-porphyrin hybrid based ratiometric bioimaging probe for Hg^{2+}: well-resolved emission spectra and unique specificity. Anal Chem 81:9993–10001. https://doi.org/10.1021/ac9018445

Li C-Y, Xu F, Li Y-F, Zhou K, Zhou Y (2012a) A fluorescent chemosensor for Hg^{2+} based on naphthalimide derivative by fluorescence enhancement in aqueous solution. Anal Chim Acta 717:122–126. https://doi.org/10.1016/j.aca.2011.12.018

Li Q, Peng M, Li H, Zhong C, Zhang L, Cheng X, Peng X, Wang Q, Qin J, Li Z (2012b) A new, "Turn-on" naphthalenedimide-based chemosensor for mercury ions with high selectivity: successful utilization of the mechanism of twisted intramolecular charge transfer, near-ir fluorescence, and cell images. Org Lett 14:2094–2097. https://doi.org/10.1021/ol300607m

Li Z, Zhou Y, Yin K, Yu Z, Li Y, Ren J (2014) A new fluorescence "turn-on" type chemosensor for Fe^{3+} based on naphthalimide and coumarin. Dyes Pigm 105:7–11. https://doi.org/10.1016/j.dyepig.2013.12.032

Li G, Gao G, Cheng J, Chen X, Zhao Y, Ye Y (2016a) Two new reversible naphthalimide-based fluorescent chemosensors for Hg^{2+}. Luminescence 31:992–996. https://doi.org/10.1002/bio.3063

Li Y, Qiu Y, Zhang J, Zhu X, Zhu B, Liu X, Zhang X, Zhang H (2016b) Naphthalimide derived fluorescent probes with turn-on response for Au^{3+} and the application for biological visualization. Biosens Bioelectron 83:334–338. https://doi.org/10.1016/j.bios.2016.04.034

Li L, Li H, Liu G, Pu S (2017) A novel fluorescent sensor for Al^{3+} based on a new diarylethene with a naphthalimide unit. J Photochem Photobiol A 338:192–200. https://doi.org/10.1016/j.jphotochem.2017.02.011

Lippert AR, New EJ, Chang CJ (2011) Reaction-based fluorescent probes for selective imaging of hydrogen sulfide in living cells. J Am Chem Soc 133:10078–10080. https://doi.org/10.1021/ja203661j

Liu J, Qian Y (2017) A novel pyridylvinyl naphthalimide-rhodamine dye: synthesis, naked-eye visible and ratiometric chemodosimeter for Hg^{2+}/Fe^{3+}. J Lumin 187:33–39. https://doi.org/10.1016/j.jlumin.2017.02.058

Liu B, Tian H (2005) A selective fluorescent ratiometric chemodosimeter for mercury ion. Chem Commun 0:3156–3158. https://doi.org/10.1039/B501913C

Liu J, Tu G, Zhou Q, Cheng Y, Geng Y, Wang L, Ma D, Jing X, Wang F (2006) Highly efficient green light emitting polyfluorene incorporated with 4-diphenylamino-1, 8-naphthalimide as green dopant. J Mater Chem 16:1431–1438. https://doi.org/10.1039/b514359d

Liu Y, Lv X, Zhao Y, Chen M, Liu J, Wang P, Guo W (2012a) A naphthalimide–rhodamine ratiometric fluorescent probe for Hg^{2+} based on fluorescence resonance energy transfer. Dyes Pigm 92:909–915. https://doi.org/10.1016/j.dyepig.2011.07.020

Liu Z, Zhang C, Wang X, He W, Guo Z (2012b) Design and synthesis of a ratiometric fluorescent chemosensor for Cu(II) with a fluorophore hybridization approach. Org Lett 14:4378–4381. https://doi.org/10.1021/ol301849z

Liu D-Y, Qi J, Liu X-Y, He H-R, Chen J-T, Yang G-M (2014) 4-Amino-1,8- naphthalimide-based fluorescent sensor with high selectivity and sensitivity for Zn^{2+} imaging in living cells. Inorg Chem Commun 43:173–178. https://doi.org/10.1016/j.inoche.2014.02.035

Liu W, Jiang J, Chen C, Tang X, Shi J, Zhang P, Zhang K, Li Z, Dou W, Yang L, Liu W (2014) Water-soluble colorimetric and ratiometric fluorescent probe for selective imaging of palladium

species in living cells. Inorg Chem 53:12590–12594. https://doi.org/10.1021/ic502223n
Liu F, Tang P, Ding R, Liao L, Wang L, Wang M, Wang J (2017a) A glycosylation strategy to develop a low toxic naphthalimide fluorescent probe for the detection of Fe^{3+} in aqueous medium. Dalton Trans 46:7515–7522. https://doi.org/10.1039/c7dt01099k
Liu X, Niu LY, Chen YZ, Yang Y, Yang QZ (2017b) A multi-emissive fluorescent probe for the discrimination of glutathione and cysteine. Biosens Bioelectron 90:403–409. https://doi.org/10.1016/j.bios.2016.06.076
Lodeiro C, Pina F (2009) Luminescent and chromogenic molecular probes based on polyamines and related compounds. Coord Chem Rev 253:1353–1383. https://doi.org/10.1016/j.ccr.2008.09.008
Lu C, Xu Z, Cui J, Zhang R, Qian X (2007) Ratiometric and highly selective fluorescent sensor for cadmium under physiological pH range: a new strategy to discriminate cadmium from zinc. J Org Chem 72:3554–3557. https://doi.org/10.1021/jo070033y
Mahato P, Saha S, Suresh E, Liddo RD, Parnigotto PP, Conconi MT, Kesharwani MK, Ganguly B, Das A (2012) Ratiometric detection of Cr^{3+} and Hg^{2+} by a naphthalimide-rhodamine based fluorescent probe. Inorg Chem 51:1769–1777. https://doi.org/10.1021/ic202073q
Marinova NV, Georgiev NI, Bojinov VB (2011) Design, synthesis and pH sensing properties of novel 1,8-naphtalimide-based bichromophoric system. J Photochem Photobiol A 222:132–140. https://doi.org/10.1016/j.jphotochem.2011.05.012
Mason WT (1999) Fluorescent and luminescent chemosensors for biological activity, 2nd edn. Academic Press, Cambridge
Mironenko AY, Tutov MV, Sergeev AA, Voznesenskiy, Bratskaya SY (2017) On/off rhodamine based fluorescent probe for detection of Au and Pd in aqueous solutions. Sens Actuators B: Chem 246:389–394. https://doi.org/10.1016/j.snb.2017.02.092
Moon JO, Choi MG, Sun T, Choe J-I, Chang S-K (2013) Synthesis of thionaphthalimides and their dual Hg^{2+}-selective signaling by desulfurization of thioimides. Dyes Pigm 96:170–175. https://doi.org/10.1016/j.dyepig.2012.08.007
Mu H, Gong R, Ma Q, Sun Y, Fu E (2007) A novel colorimetric and fluorescent chemosensor: synthesis and selective detection for Cu^{2+} and Hg^{2+}. Tetrahedron Lett 48:5525–5529. https://doi.org/10.1016/j.tetlet.2007.05.155
Nandhikonda P, Begaye MP, Heagy MD (2009) Highly water-soluble, OFF–ON, dual fluorescent probes for sodium and potassium ions. Tetrahedron Lett 50:2459–2461. https://doi.org/10.1016/j.tetlet.2009.02.197
Ott I, Xu Y, Liu J, Kokoschka M, Harlos M, Sheldrick W, Qian X (2008) Sulfur-substituted naphthalimides as photoactivatable anticancer agents: DNA interaction, fluorescence imaging, and phototoxic effects in cultured tumor cells. Bioorg Med Chem 16:7107–7116. https://doi.org/10.1016/j.bmc.2008.06.052
Panchenko PA, Fedorov YV, Perevalov VP, Jonusauskas G, Fedorova OA (2010) Cation-dependent fluorescent properties of naphthalimide derivatives with N-benzocrown ether fragment. J Phys Chem A 114:4118–4122. https://doi.org/10.1021/jp103728
Papalia T, Barattucci A, Barreca D, Bellocco E, Bonaccorsi P, Minuti L, Nicolo MS, Temperini A, Foti C (2017) Sequestering ability to Cu^{2+} of a new bodipy-based dye and its behavior as in vitro fluorescent sensor. J Inorg Biochem 167:116–123. https://doi.org/10.1016/j.jinorgbio.2016.11.030
Parkesh R, Lee TC, Gunnlaugsson T (2007) Highly selective 4-amino-1, 8-naphthalimide based fluorescent photoinduced electron transfer (PET) chemosensors for Zn(II) under physiological pH conditions. Org Biomol Chem 5:310–317. https://doi.org/10.1039/B614529A
Parkesh R, Veale EB, Gunnlaugsson T (2011) Fluorescent Detection Principles and Strategies. In: Wang B, Anslyn EV (eds) Chemosensors principles, strategies, and applications, Chap 12. Wiley, Hoboken, New Jersey, pp 229–252
Que EL, Domaille DW, Chang CJ (2008) Metals in neurobiology: probing their chemistry and biology with molecular imaging. Chem Rev 108:1517–1549. https://doi.org/10.1021/cr078203u
Ramasamy K, Thambusamy S (2017) Dual emission and pH based naphthalimide derivative fluorescent sensor for the detection of Bi^{3+}. Sens Actuators B: Chem 247:632–640. https://doi.org/10.1016/j.snb.2017.03.043
Rurack K, Resch-Genger U, Bricks JL, Spieles M (2000) Cation-triggered 'switching on' of the red/near infra-red (NIR) fluorescence of rigid fluorophore–spacer–receptor ionophores. Chem Commun 0:2103–2104. https://doi.org/10.1039/B006430K
Saini A, Singh J, Kaur R, Singh N, Kaur N (2014) Naphthalimide-based organic nanoparticles for aluminium recognition in acidic soil and aqueous media. New J Chem 38:4580–4586. https://doi.org/10.1039/C4NJ00473F
Saura AV, Burguete MI, Galindo F, Luis SV (2017) Novel fluorescent anthracene–bodipy dyads displaying sensitivity to pH and turn-on behaviour towards Cu(II) ions. Org Biomol Chem 15:3013–3024. https://doi.org/10.1039/C7OB00274B
Shaki H, Gharanjiga K, Rouhani S, Khosravi A (2010) Synthesis and photophysical properties of some novel fluorescent dyes based on naphthalimide derivatives. J Photochem Photobiol, A 216:44–50. https://doi.org/10.1016/j.jphotochem.2010.09.004
Shao X, Kang R, Zhang Y, Huang Z, Peng F, Zhang J, Wang Y, Pan F, Zhang W, Zhao W (2015) Highly selective and sensitive 1-amino BODIPY-based red fluorescent probe for thiophenols with high off-to-on contrast ratio. Anal Chem 87:399–405. https://doi.org/10.1021/ac5028947
Sharma H, Kaur N, Singh N (2012) Imine linked 1, 8-naphthalimide: chromogenic recognition of metal ions, density function theory and cytotoxic activity. Inorg Chimica Acta 391:83–87. https://doi.org/10.1016/j.ica.2012.05.003
Staneva D, Grabchev I, Soumillion J-P, Bojinov V (2007) Pteridine-based fluorescent pH sensors designed for physiological applications. J Photochem Photobiol A: Chem 189:192–197. https://doi.org/10.1016/j.jphotochem.2012.08.002
Staneva D, Bosch P, Grabchev I (2012) Ultrasonic synthesis and spectral characterization of a new blue fluorescent dendrimer as highly selective chemosensor for Fe^{3+} cations. J Mol Struct 1015:1–5. https://doi.org/10.1016/j.molstruc.2012.02.010
Stewart WW (1981) Synthesis of 3, 6-disulfonated 4-aminonaphthalimides. J Am Chem Soc 103:7615–7620. https://doi.org/10.1021/ja00415a033
Sun S, Hu W, Gao H, Qi H, Ding L (2017) Luminescence of ferrocene-modified pyrene derivatives for turn-on sensing of Cu^{2+} and anions. Spectrochima Acta Mol Biomol Spectrosc 184:30–37. https://doi.org/10.1016/j.saa.2017.04.073
Tamanini E, Katewa A, Sedger LM, Todd MH, Watkinson M (2009) A synthetically simple, click-generated cyclam-based zinc (II) sensor. Inorg Chem 48:319–324. https://doi.org/10.1021/ic8017634
Tamanini E, Flavin K, Motevalli M, Piperno S, Gheber LA, Todd MH, Watkinson M (2010) Cyclam-based "clickates": homogeneous and heterogeneous fluorescent sensors for Zn(II). Inorg Chem 49:3789–3800. https://doi.org/10.1021/ic901939x
Un H-I, Huang C-B, Huang C, Jia T, Zhao X-L, Wang C-H, Xu L, Yang H-B (2014a) A versatile fluorescent dye based on naphthalimide: highly selective detection of Hg^{2+} in aqueous solution and living cells and its aggregation-induced emission. Org Chemistry Frontiers 1:1083–1090. https://doi.org/10.1039/C4QO00185K
Un HI, Huang CB, Huang J, Huang C, Jia T, Xu L (2014b) A Naphthalimide-based fluorescence "Turn-On" probe for the detection of

Pb2 + in aqueous solution and living cells. Chemistry 9:3397–3402. https://doi.org/10.1002/asia.201402946

Valeur B, Leray I (2001) PCT (Photoinduced Charge Transfer) fluorescent molecular sensors for cation recognition. In: Valeur B, Brochon JC (eds) New Trends in Fluorescence Spectroscopy, vol 1. Springer, Berlin, pp 187–207

Vonlanthen M, Connelly CM, Deiters A, Linden A, Finney NS (2014) Thiourea-based fluorescent chemosensors for aqueous metal ion detection and cellular imaging. J Org Chem 79:6054–6060. https://doi.org/10.1021/jo500710g

Wang J, Xiao Y, Zhang Z, Qian X, Yang Y, Xu Q (2005) A pH-resistant Zn (II) sensor derived from 4-aminonaphthalimide: design, synthesis and intracellular applications. J Mater Chem 15:2836–2839. https://doi.org/10.1039/B500766F

Wang C, Zheng X, Huang R, Yan S, Xie X, Tian T, Huang S, Weng X, Zhou X (2012) A 4-Amino-1, 8-naphthalimide derivative for selective fluorescent detection of palladium (ii) ions. Asian J Org Chem 1:259–263. https://doi.org/10.1002/ajoc.201200061

Wang F, Xu Y, Aderinto SO, Peng H, Zhang H, Wu H (2017) A new highly effective fluorescent probe for Al^{3+} ions and its application in practical samples. J Photochem Photobiol A 332:273–282. https://doi.org/10.1016/j.jphotochem.2016.09.004

Wasielewski MR (1992) Photoinduced electron transfer in supramolecular systems for artificial photosynthesis. Chem Rev 92(3):435–461. https://doi.org/10.1021/cr00011a005

Wei T, Wang J, Chen Y, Han Y (2015) Combining the PeT and ICT mechanisms into one chemosensor for the highly sensitive and selective detection of zinc. RSC Adv 5:57141–57146. https://doi.org/10.1039/C5RA11194C

Wu X-F, Ma Q-J, Wei X-J, Hou Y-M, Zhu X (2013) A selective fluorescent sensor for Hg^{2+} based on covalently immobilized naphthalimide derivative. Sens Actuators B: Chem 183:565–573. https://doi.org/10.1016/j.snb.2013.04.024

Wu S, Zhang K, Wang Y, Mao D, Liu X, Yu J, Wang L (2014) A novel Cr^{3+} turn-on probebased on naphthalimide and BINOL framework. Tetrahedron Lett 55:351–353. https://doi.org/10.1016/j.tetlet.2013.11.024

Xiao Y, Rowe AA, Plaxco KW (2007) Electrochemical detection of parts-per-billion lead via an electrode-bound DNAzyme assembly. J Am Chem Soc 129:262–263. https://doi.org/10.1021/ja067278x

Xu Z, Qian X, Cui J (2005) Colorimetric and ratiometric fluorescent chemosensor with a large red-shift in emission: Cu(II)-only sensing by deprotonation of secondary amines as receptor conjugated to naphthalimide fluorophore. Org Lett 7:3029–3032. https://doi.org/10.1021/ol051131d

Xu Z, Qian X, Cui J, Zhang R (2006) Exploiting the deprotonation mechanism for the design of ratiometric and colorimetric Zn^{2+} fluorescent chemosensor with a large red-shift in emission. Tetrahedron 62:10117–10122. https://doi.org/10.1016/j.tet.2006.08.050

Xu Z, Han SJ, Lee C, Yoon J, Spring DR (2010a) Development of off–on fluorescent probes for heavy and transition metal ions. Chem Commun 46:1679–1681. https://doi.org/10.1039/B924503K

Xu Z, Pan J, Spring DR, Cui J, Yoon J (2010b) Ratiometric fluorescent and colorimetric sensors for Cu^{2+} based on 4,5-disubstituted-1,8-naphthalimide and sensing cyanide via Cu^{2+} displacement approach. Tetrahedron 66:1678–1683. https://doi.org/10.1016/j.tet.2010.01.008

Xu Z, Yoon J, Spring DR (2010c) Fluorescent chemosensors for Zn^{2+}. Chem Soc Rev 39:1996–2006. https://doi.org/10.1039/B916287A

Xu Z, Yoon J, Spring DR (2010d) A selective and ratiometric Cu^{2+} fluorescent probe based on naphthalimide excimer–monomer switching. Chem Commun 46:2563–2565. https://doi.org/10.1039/C000441C

Xu Z, Zheng S, Yoon J, Spring DR (2010e) Discovery of a highly selective turn-on fluorescent probe for Ag^{+}. Analyst 135:2554–2559. https://doi.org/10.1039/C0AN00405G

Xu J-H, Hou Y-M, Ma Q-J, Wu X-F, Wei X-J (2013) A highly selective fluorescent sensor for Fe^{3+} based on covalently immobilized derivative of naphthalimide. Spectrochima Acta Mol Biomol Spectrosc 112:116–124. https://doi.org/10.1016/j.saa.2013.04.044

Xu Y, Aderinto SO, Wu H, Peng H, Zhang H, Zhang J, Fan X (2017) A highly selective fluorescent chemosensor based on naphthalimide and schiff base units for Cu^{2+} detection in aqueous medium. Z Naturforsch B Chemical Science 72:35–43. https://doi.org/10.1515/znb-2016-0138

Xue D, Zheng C, Fan C, Liu G, Pu S (2015) A colorimetric fluorescent sensor for Cr^{3+} based on a novel diarylethene with a naphthalimide-rhodamine B group. J Photochem Photobiol A Chem 303–304:59–66. https://doi.org/10.1016/j.jphotochem.2015.02.006

Yang R, Guo X, Wang W, Zhang Y, Jia L (2012) Highly selective and sensitive chemosensor for Hg^{2+} based on the naphthalimide fluorophore. J Fluoresc 22:1065–1071. https://doi.org/10.1007/s10895-012-1044-2

Yang L, Yang W, Xu D, Zhang Z, Liu A (2013) A highly selective and sensitive Fe^{3+} fluorescent sensor by assembling three 1, 8-naphthalimide fluorophores with a tris (aminoethylamine) ligand. Dyes Pigm 97:168–174. https://doi.org/10.1016/j.dyepig.2012.12.016

Yu C, Zhang J (2014) Copper (II)-Responsive "Off-On" chemosensor based on a naphthalimide derivative. Asian J Org Chem 3:1312–1316. https://doi.org/10.1002/ajoc.201402160

Yu C, Chen L, Zhang J, Li J, Liu P, Wang W, Yan B (2011) "Off-On" based fluorescent chemosensor for Cu^{2+} in aqueous media and living cells. Talanta 85:1627–1633. https://doi.org/10.1016/j.talanta.2011.06.057

Yu C, Zhang J, Ding M, Chen L (2012) Silver (I) ion detection in aqueous media based on "off-on" fluorescent probe. Anal Methods 4:342–344. https://doi.org/10.1039/C2AY05714J

Yu C, Wen Y, Qin X, Zhang J (2014) A fluorescent ratiometric Cu^{2+} probe based on FRET by naphthalimide-appended rhodamine derivatives. Anal Methods 6:9825–9830. https://doi.org/10.1039/C4AY01863J

Yu M, Du W, Zhou W, Liu C, Wei L, Zhang H (2016) A 1,8-naphthalimide-based chemosensor with an off-on fluorescence and lifetime imaging response for intracellular Cr^{3+} and further for S^{2-}. Dyes Pigm 126:279–285. https://doi.org/10.1016/j.dyepig.2015.12.001

Zhang JF, Zhou Y, Yoon J, Kim Y, Kim SJ, Kim JS (2010) Naphthalimide modified rhodamine derivative: ratiometric and selective fluorescent sensor for Cu^{2+} based on two different approaches. Org Lett 12:3852–3855. https://doi.org/10.1021/ol101535s

Zhang JF, Kim S, Han JH, Lee S-J, Pradhan T, Cao QY, Lee SJ, Kang C, Kim SJ (2011a) Pyrophosphate-selective fluorescent chemosensor based on 1, 8-naphthalimide–DPA–Zn(II) complex and its application for cell imaging. Org Lett 13:5294–5297. https://doi.org/10.1021/ol202159x

Zhang JF, Zhou Y, Yoon J, Kim JS (2011b) Recent progress in fluorescent and colorimetric chemosensors for detection of precious metal ions (silver, gold and platinum ions). Chem Soc Rev 40:3416–3429. https://doi.org/10.1039/C1CS15028F

Zhang J, Yu C, Lu G, Fu Q, Li N, Ji Y (2012) A Ag^{+}-selective "off–on" probe based on a naphthalimide derivative. New J Chem 36:819–822. https://doi.org/10.1039/C2NJ20974H

Zhang C, Liu Z, Li Y, He W, Gao X, Guo Z (2013a) In vitro and in vivo imaging application of a 1, 8-naphthalimide-derived Zn^{2+}

fluorescent sensor with nuclear envelope penetrability. Chem Commun 49:11430–11432. https://doi.org/10.1039/c3cc46862c

Zhang Z, Chen Y, Xu D, Yang L, Liu A (2013b) A new 1, 8-naphthalimide-based colorimetric and "turn-on" fluorescent Hg^{2+} sensor. Spectrochima Acta Mol Biomol Spectrosc 105:8–13. https://doi.org/10.1016/j.saa.2012.11.113

Zhang X, Yin J, Yoon J (2014a) Recent advances in development of chiral fluorescent and colorimetric sensors. Chem Rev 114(9):4918–4959. https://doi.org/10.1021/cr400568b

Zhang Z, Lu S, Sha C, Xu D (2014b) A single thiourea-appended 1,8-naphthalimide chemosensor for three heavy metal ions: Fe^{3+}, Pb^{2+}, and Hg^{2+}. Sens Actuators B: Chem 208:258–266. https://doi.org/10.1016/j.snb.2014.10.136

Zhang Y-M, Zhong K-P, Su J-X, Chen X-P, Yao H, Wei T-B, Lin Q (2017) A novel histidine-functionalized 1, 8-naphthalimide-based fluorescent chemosensor for the selective and sensitive detection of Hg^{2+} in water. New J Chem 41:3303–3307. https://doi.org/10.1039/C6NJ03930H

Zhao LY, Mi QL, Wang GK, Chen JH, Zhang JF, Zhao QH, Zhou Y (2013) 1, 8-Naphthalimide-based 'turn-on' fluorescent sensor for the detection of zinc ion in aqueous media and its applications for bioimaging. Tetrahedron Lett 54:3353–3358. https://doi.org/10.1016/j.tetlet.2013.04.045

Zhou Y, Zhou H, Ma T, Zhang J, Niu J (2012) A new Schiff base based on vanillin and naphthalimide as a fluorescent probe for Ag^{+} in aqueous solution. Spectrochima Acta Mol Biomol Spectrosc 88:56–59. https://doi.org/10.1016/j.saa.2011.11.054

Zhu W, Hu M, Yao R, Tian H (2003) A novel family of twisted molecular luminescent materials containing carbazole unit for single-layer organic electroluminescent devices. J Photochem Photobiol A Chem 154:169–177. https://doi.org/10.1016/S1010-6030(02)00325-8